How to cite: *Angew. Chem. Int. Ed.* **2022**, *61*, e202107537
International Edition: doi.org/10.1002/anie.202107537
German Edition: doi.org/10.1002/ange.202107537

Multiphase Microreactors

Multiphase Microreactors Based on Liquid–Liquid and Gas–Liquid Dispersions Stabilized by Colloidal Catalytic Particles

*Dmytro Dedovets, Qingyuan Li, Loïc Leclercq, Veronique Nardello-Rataj, Jacques Leng, Shuangliang Zhao, and Marc Pera-Titus**

Pickering emulsions, foams, bubbles, and marbles are dispersions of two immiscible liquids or of a liquid and a gas stabilized by surface-active colloidal particles. These systems can be used for engineering liquid–liquid–solid and gas–liquid–solid microreactors for multiphase reactions. They constitute original platforms for reengineering multiphase reactors towards a higher degree of sustainability. This Review provides a systematic overview on the recent progress of liquid–liquid and gas–liquid dispersions stabilized by solid particles as microreactors for engineering eco-efficient reactions, with emphasis on biobased reagents. Physicochemical driving parameters, challenges, and strategies to (de)stabilize dispersions for product recovery/catalyst recycling are discussed. Advanced concepts such as cascade and continuous flow reactions, compartmentalization of incompatible reagents, and multiscale computational methods for accelerating particle discovery are also addressed.

From the Contents

1. Introduction

Multiphase reactions combining two immiscible phases and a solid catalyst are widespread in the chemical industry. Liquid–liquid–solid (L-L-S) reactions are commonly carried out in mechanically stirred tank reactors operating in batch, semibatch, or continuous mode,[1] whereas gas–liquid–solid (G-L-S) reactions are operated in packed beds (e.g., trickle beds, bubble columns), slurry reactors, and fluidized beds.[1b,2] (A list of abbreviations is provided at the end of the Review for ready reference.) These technologies often suffer from inhomogeneous mixing and mass/heat transfer limitations due to low L-L, G-L, and L-S interfacial areas, especially for fast reactions.

Particle-stabilized L-L and G-L dispersions based on emulsions, foams, bubbles, liquid marbles, and bijels can be employed as microreactors for multiphase reactions. These systems combine the advantages of homogeneous and heterogeneous catalysts: high activity and selectivity, easy phase separation, catalyst reuse, and compartmentalization of reactants and products. Unlike conventional reactors, L-L-S and G-L-S microreactors can offer enhanced catalytic properties by a refined engineering of the three-phase contact at the nanoscale. These unique systems can be used as a platform for reengineering multiphase reactors towards a higher degree of sustainability.

In 2015, we published a Minireview on emerging applications of particle-stabilized emulsions for interfacial reactions,[3] which was updated by Bago and Binks, mostly focusing on enzymes.[4] The field has been recently boosted with innovative applications, and concepts based on L-L and G-L dispersions have emerged with credentials for sustainable chemistry and catalysis. Herein, we provide a critical survey of L-L-S and G-L-S microreactors for engineering eco-efficient reactions using biobased reagents, with an emphasis on catalyst design. We also point the main directions to advance the state of the art, and the benefits of multiscale computational methods for assisting and accelerating the development of novel surface-active particles, catalytic systems, and microreactors.

2. Particle-Stabilized L-L and G-L Dispersions

Colloidal particles (Figure 1a) can irreversibly adsorb at L-L[5] and G-L[6] interfaces generating a film, which can arise from few particles to a dense multilayer structure acting as a mechanical barrier against coarsening. Typically, surface-

[*] Dr. D. Dedovets, Dr. Q. Li, Prof. M. Pera-Titus
Eco-Efficient Products and Processes Laboratory (E2P2L)
UMI 3464 CNRS-Solvay
3966 Jin Du Road, Xin Zhuang Ind Zone, 201108 Shanghai (China)
E-mail: marc.pera-titus-ext@solvay.com
Dr. D. Dedovets, Dr. J. Leng
Laboratoire du Futur (LOF), UMR 5258
CNRS-Solvay-Universite Bordeaux 1
178 Av Dr Albert Schweitzer, 33608 Pessac Cedex (France)
Dr. L. Leclercq, Prof. V. Nardello-Rataj
Univ Lille, CNRS, Centrale Lille, Univ Artois
UMR 8181 UCCS
F-59000 Lille (France)
Prof. S.-L. Zhao
Guangxi Key Laboratory of Petrochemical Resource Processing and Process Intensification Technology
School of Chemistry and Chemical Engineering
Guangxi University, 530004 Nanning (China)
Prof. M. Pera-Titus
Cardiff Catalysis Institute, School of Chemistry, Cardiff University
Main Building, Park Place, Cardiff CF10 3AT (UK)
Supporting information and the ORCID identification numbers for the authors of this article can be found under: https://doi.org/10.1002/anie.202107537.

active particles possess hydrophilic/hydrophobic functions, usually randomly distributed, one of which ensures particle dispersion, while the other allows partial wetting by the second phase. The different functions can be physically separated on the particle, as commonly found in Janus particles.[7] This is the case for particles with one-half surface composed of hydrophilic groups and the other half of hydrophobic groups.[8] Besides, the particle size, shape (e.g., spheres, nanofibers, nanotubes, nanosheets),[9] roughness, and fractal dimension determine the wetting properties and stability of L-L[10] and G-L dispersions.[11] Overall, the particle design defines the interfacial contact angle, θ (Figure 1b), which is a primary descriptor of L-L and G-L dispersions: 1) thermodynamic stability (minimum energy of particle desorption ΔG_d reaches a maximum when $\theta = 90°$), 2) interfacial adsorption kinetics of particles, and 3) local microenvironment near the catalytic centers (see the Supporting Information and Figures S1–S4 for details).

Given two immiscible phases, a variety of L-L and G-L dispersions can be stabilized by colloidal particles (Figure 1b).[12] Targeting microreactors, the most attractive dispersions are Pickering emulsions (L_1/L_2), multiple emulsions, and bicontinuous jammed emulsion gels (bjiels) ($L_1/L_2/L_1$), bubbles (G/L), liquid foams (G/L), and liquid marbles (L/G), showing potential interconversion (e.g., by catastrophic phase inversion) (Figure 1b). More complex systems comprise emulsion-based marbles and bubbles encapsulated in liquid marbles, affording compartmentalization.[13] For a given particle, the contact angle and concentration of particles, along with the nature and volume ratio of the immiscible phases, control the type of dispersion, stability, and size of droplets/bubbles (Figure 1b,c).[12] In particular, oil foams usually demand particles with low-surface energy (e.g., fluorinated particles)[14] and Janus particles.[15] Hydrophobic particles can be used to prepare water and ionic liquid marbles,[16] while oleophobic particles stabilize marbles based on organic solvents.[17] Fluorinated silicas are versatile for stabilizing non-aqueous marbles arising from apolar hydrocarbons and polar oils to glycerol.[18]

Pickering L-L and G-L dispersions exhibit similar stabilization mechanisms. However, some differences are at play, which impact their applications in catalysis.[19] G-L dispersions are more compressible than liquid droplets, favoring their deformation from individual bubbles into polyhedral structures.[20] Besides, the object size is much larger in foams/marbles (10 μm–5 mm) than in emulsions (10–100 μm). Particle-stabilized L-L and G-L dispersions are much more stable than surfactant-stabilized counterparts, since primary destabilization mechanisms can be discouraged. Foam instability occurs by film drainage, coalescence, and rupture, while instability in emulsions also occurs by creaming and sedimentation, which are induced by gravity.[21] In most cases, droplets can be redispersed again as they do not coalesce due to the formation of a shell with irreversibly adsorbed particles.

Flocculation often occurs in L-L and G-L dispersions, where droplets/bubbles remain as aggregates or clusters, stabilizing the systems.[21] In G-L systems, bubble disproportionation due to gas diffusion within the particle shell can be a source of instability, resulting in the shrinking of smaller and growth of larger bubbles.[22] A similar phenomenon (i.e. Ostwald ripening) occurs in emulsions but is only relevant when very small droplets (< 0.1 μm) are present.[21] Interdroplet networks can stabilize emulsions,[23] whereas a particle network between adsorbed and non-adsorbed particles can occur in aqueous foams, reducing film drainage between bubbles.[24]

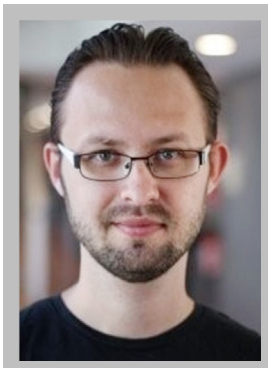

Dmytro Dedovets received a MSc degree in Chemical Engineering (2007) at Donetsk National Technical University (Ukraine) and a PhD (2014) in Physical Chemistry at University of Bordeaux (France). He conducted postdoctoral research in joint academic/industrial laboratories with CEA, Saint-Gobain, and Solvay on the formulation of surfactants, polymers, and particle-stabilized foams and emulsions and their use as functional materials.

Loïc Leclercq received a MSc degree in Chemistry (Université d'Artois, 2003) and Organic and Macromolecular Chemistry (Université de Lille, 2004). In 2007, he earned his PhD at Université de Lille and joined the Université de Montréal (Canada) as a postdoctoral researcher. Since 2008, he has been Assistant Professor at Université de Lille (France). His research interests include catalysis, supramolecular chemistry, pharmaceutical formulation, and the history of chemistry.

Qingyuan Li obtained his PhD in Chemical Engineering and Technology from Beijing University of Chemical Technology in 2014. He conducted postdoctoral research at Tsinghua University on hydrogenation reactions of tetrachlorosilanes. He has also worked as a research associate at Korea University of Technology and Education, E2P2L (CNRS-Solvay), and West Virginia University. His current research focuses on organosilicon/polysilicon synthesis, catalysis, and engineering.

Véronique Rataj is Professor at Centrale Lille Institute. She received an engineering degree from the School ESCOM (Paris, France) and earned her PhD in 1996 at University of Lille. After postdoctoral research at DSM in The Netherlands, she joined the University of Lille as Assistant Professor in 2000. She is the leader of the Research group Colloids Catalysis Oxidation (CÏSCO) and Deputy Director of the Laboratory UCCS UMR 8181. Her research interests include formulation science, supramolecular chemistry, and the chemistry and physicochemistry of dispersed systems, oxidation, and fragrances.

3. Genesis of Particle-Stabilized L-L and G-L Dispersions

The state-of-the-art techniques for preparing surfactant-stabilized emulsions/foams can be transposed to particle-stabilized counterparts (Figure 1d, Table S1).[25] The most frequently used techniques comprise rotor-stator and high-pressure homogenization, and sonication. They allow high-rate production but can suffer from particle/substrate degradation due to intensive shear or high temperature. Microfluidics (MF) using flow-focusing geometries, coaxial, T-junction, and double coaxial injection can generate monodisperse dispersions with fine control of shell properties (Table 1).[26] Colloidal particles in MF devices show three limitations: 1) clogging due to low dispersion/wetting, 2) slow adsorption kinetics, and 3) particle adsorption on microchannel walls. Current MF methods for stabilizing emulsions/foams offer a tradeoff between slow bubble/droplet production rate and particle excess.

Clogging can be discouraged by using pH-sensitive particles (Figure S5a,b). Dissolution of CO_2 bubbles can induce a pH change, which renders well-dispersed particles (e.g., polystyrene/acrylic acid, carboxylated silica) more hydrophobic, forcing them to the G-L interface.[6a,27] Also, a transient double-emulsion approach can be implemented using a T-junction to generate emulsions with controlled surface coverage (Figure S5c).[28] The particles are dispersed in the middle phase, which dissolves in either the inner or outer phases leaving particles at the interface between both phases. Using this method, composite shells using particles with different or even opposite adsorption properties can be produced.[29]

Particle adsorption kinetics is key for preparing emulsions/foams in MF devices. Indeed, the particle concentration near the interface and the shear stress during droplet formation are critical parameters for stabilizing emulsions. Sonication-coupled devices have been developed to accelerate particle adsorption for fabricating bubbles (Figure S5d).[30] Also, the droplet production junction can be designed to reduce the stabilization time and minimize the particle excess (Figure S5e).[31] Surface treatment of chips (e.g., polymer coating, organosilane grafting, photolithography) can prevent particle accumulation in channel constrictions. Along with emulsion and foam generation, MF offers a range of analytical capabilities for characterizing the interfacial particle assembly (Figure S6).

Liquid marbles are commonly prepared by manual rolling of liquid droplets on a hydrophobic powder bed in an inclined surface (Figure 1e, Table 1).[17a] The liquid can also be sprayed or dripped from a syringe, where a drop recoil generates a fluid flow entraining the powder and forming the shell.[56] Modification of this method allows marble production by electrohydrodynamic pulling.[57] A needle syringe filled with liquid serves as the anode, while a motorized micrometer stage dispenses the liquid at a fixed rate. An electric field is applied to detach the droplet at a desired volume. The marbles are formed by impact of the droplet on a powder bed placed between the needle and an Al plate serving as cathode. Alternatively, highly charged particles in a packed bed migrate to an oppositely charged liquid droplet, resulting in a spontaneous electrostatic assembly of a particle shell.[58] Droplet evaporation from the surface of a hydrophobic granular material can result in the formation of temporary liquid marbles.[59] Liquid marble production by sonication was also demonstrated: oleic acid is added to a glass vial filled

Jacques Leng is a CNRS scientist and the deputy director of the Laboratory of the Future (Bordeaux). He is an expert in non-equilibrium soft matter, chemical engineering, microfluidics, and materials. He has developed innovative tools based on microfluidics for preparing materials applied to optics and acoustics, and for applications in chemistry and optofluidics. His current research focuses on 3D printing of soft matter.

Shuangliang Zhao is a professor of Chemical Engineering at Guangxi University. He received his PhD in physical chemistry from the École normale supérieure de Lyon (France) in 2007, and then carried out postdoctoral research at the École normale supérieure (Paris) and the University of California at Riverside (USA). In 2012, he joined the East China University of Science and Technology in Shanghai, and was promoted to professor in 2017. His research focuses on structured thermodynamics and micro/nanochemical engineering.

Marc Pera-Titus is professor and chair in sustainable catalytic chemistry at Cardiff University (UK). He received a double MSc degree in Chemical Engineering (2001) and Physical Chemistry (2002), and a PhD (2006) from University of Barcelona (Spain). In 2007, he joined IRCELYON/CNRS (France) as a postdoc and was further appointed CNRS fellow in 2008. From 2011–2020, he was project leader, expert, and deputy director at the E2P2L CNRS-Solvay (Shanghai, China). He is interested in membranes, adsorption, catalysis, and process eco-design.

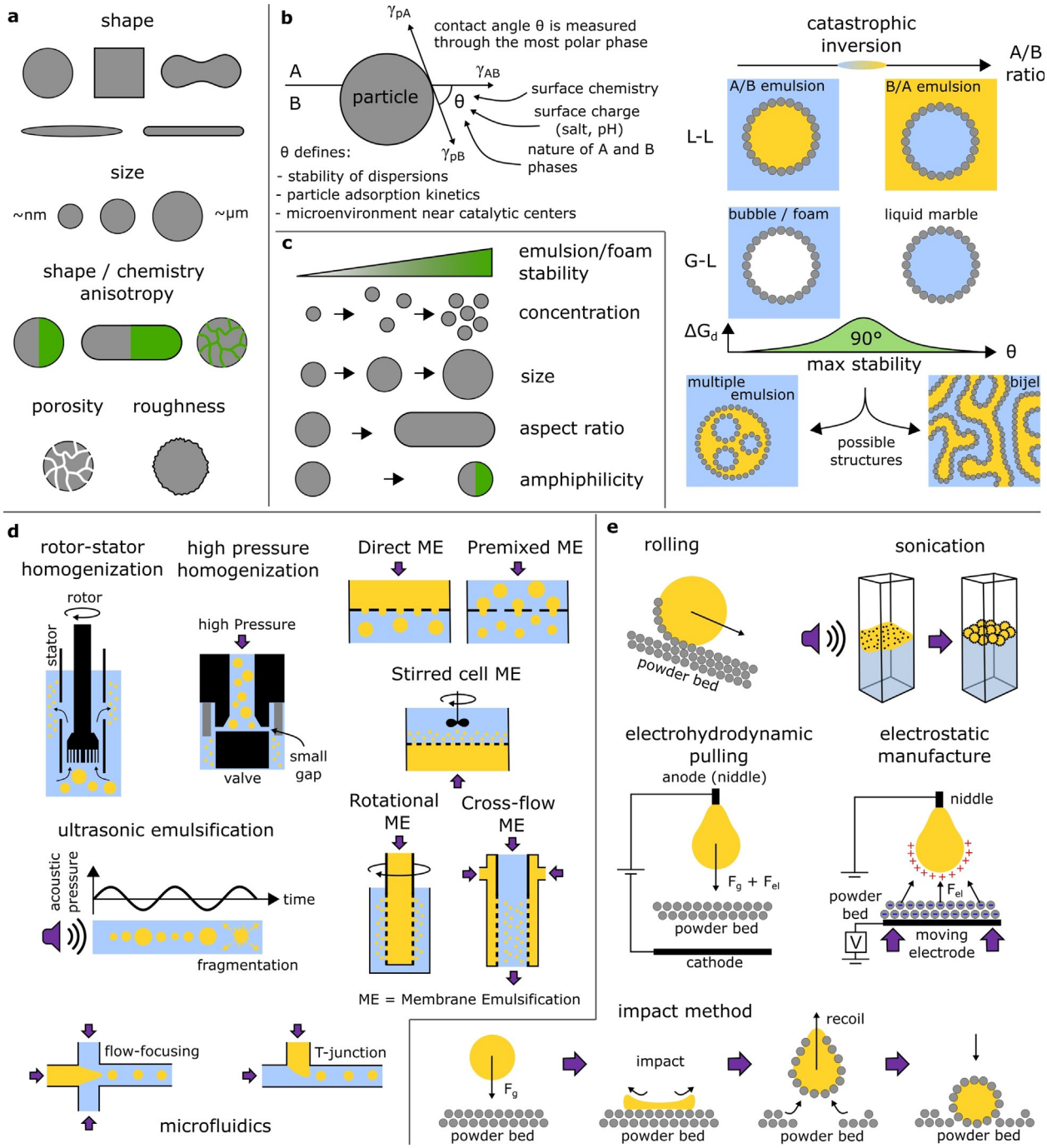

Figure 1. Particle-stabilized L-L and G-L dispersions and preparation strategies: a) main properties of surface-active particles; b) interfacial contact angle and relevant dispersions for engineering L-L-S and G-L-S microreactors; c) main parameters affecting emulsion/foam stability; d) methods for preparing emulsions and foams; e) methods for preparing liquid marbles.

with water followed by Ag powder in a sonication bath.[60] Finally, dry water can be prepared using a high-shear vertical axis mixer equipped with knife blades, affording 98 wt% water encapsulation.[61]

4. Catalysis in Particle-Stabilized L-L-S and G-L-S Microreactors

L-L-S and G-L-S microreactors can be engineered using two main approaches: 1) Pickering assisted catalysis (PAC), where a homogeneous catalyst or enzyme is combined with particles, colloidosomes, polymersomes, or microgels forming emulsions, and 2) Pickering interfacial catalysis (PIC), where

Table 1: Summary of particle-stabilized L/L and G/L dispersions generated using MF devices.

Particle core	Surface groups	Particle size	Conc.	Additives	Stimuli	System type	Object diameter	Chip type, material	Ref.
silica	-OH	5–150 nm	not reported	polymer/PLS	pH	FG/W + P	3–9 μm	flow focusing, PDMS	[32]
silica	-OH	22 nm	1–10 wt%	surfactant (*n*-amylamine)	–	G/W + P	500 μm	T-junction, glass capillary	[33]
silica	-OH	12 nm	2, 10 wt%	surfactant (CTAB)	–	G/W + P	slug bubble	T-junction, PDMS	[34]
ethyl cellulose	-OH, $-OCH_2CH_3$	100–300 nm	1 wt%	citric acid (pH 3)	ultrasound	G/W + P	10 μm	flow focusing, glass	[30]
PS; silica	-COOH, phenyl	2.8–3.5 μm 20 nm (silica)	0–5 wt%	NaOH (pH 14)	pH	G/W + P	50–70 μm	T-junction, PDMS	[27]
PS	-COOH, phenyl	2.8 μm	1.2 wt%	NaOH (pH 14)	T, pH	G/W + P	43–115 μm	flow focusing, PDMS	[35]
PS	-COOH, phenyl	0.5, 1, 4.5 μm	0.1–1 wt%	0.5 M NaCl	–	G/W + P	slug bubble	other, PDMS	[36]
PS	-COOH, phenyl	0.5, 1, 4.5 μm	0.5 wt%	0.5 M NaCl	–	G/W + P	10–100 μm	other, PDMS	[37]
PS	charged group,* phenyl	1–4.6 μm	0.1 vol%	–	–	G/W + P	400 μm	flow focusing, not reported	[38]
silica	not reported	15 nm	28 wt%	PVA (in water)	–	G/O + P/W	30–80 μm	flow focusing, glass capillary	[39]
polyamide	amide backbone	30 μm	–	–	–	W/G + P or O/G + P or FO/G + P	slug droplet	rect. channel, glass capillary	[40]
clay	-ONa	nanofluid	0.5, 1, 1.5 wt%	0.05, 0.1, and 0.5 M NaCl	–	O/W + P	80–120 μm	T-junction, glass chip	[41]
silica	-OH	5–30 nm (6.5 μm)**	0.4 wt%	(pH 5.8)	–	O/W + P	50–100 μm	EDGE, silicon	[42]
silica	$-NH_2$, -OH,	0.5–1 μm	3–3.4%	–	–	W + P/O	130 μm	flow focusing, PDMS	[43]
PS	$-SO_4$, phenyl	100, 200, 300 nm	0.125–1 wt%	0.1 M KCl	–	O/W + P	300 μm	flow focusing, glass capillary	[44]
PS	-COOH, phenyl	1, 6, 10 μm	2–27×10^6 part mL^{-1}	polymers (dextran/PEG)	–	W/W + P	100 μm	flow focusing, PDMS	[45]
PS	-COOH, phenyl	3.5 μm	4–16 wt%	EtOH (15:85 v/v in water)	–	W + P/O	40–100 μm	flow focusing, PDMS	[46]
various	various	1–4.6 μm	0.1 vol%	–	–	O/W + P	various	flow focusing, not reported	[38]
PNIPAm	acrylamide isopropyl	–	1.4 wt%	glutaraldehyde (1 vol% in water) DC547 surfactant (0.4 wt% in oil)	–	W + P/O	80 μm	flow focusing, glass capillary	[47]
tripalmitin	sodium caseinate	170 nm	0.005–5%	–	–	O/W + P	57–96 μm	T-junction, glass chip	[48]
silica	-C16, -OH	12 nm	0.2–0.6 wt%	–	–	O/W + P	22–30 μm	flow focusing, glass chip	[49]

Table 1: (Continued)

Particle core	Surface groups	Particle size	Conc.	Additives	Stimuli	System type	Object diameter	Chip type, material	Ref.
silica	TMS, -OH	7.1 nm	0–5 $g\,L^{-1}$	0–0.3 M NaCl	–	FO/W + P	44 μm	flow focusing, PDMS	[50]
silica	perfluorooctyl, -OH	780 nm	4 wt%	–	–	W/FO + P	30–40 μm	flow focusing, not reported	[51]
silica	perfluorooctyl, -OH	94 nm	6 $mg\,mL^{-1}$	–	–	W/FO + P	80 μm	other, PDMS	[52]
silica	perfluorooctyl, -OH	65 nm	1–12 $mg\,mL^{-1}$	–	–	W/FO + P	–	flow focusing, PDMS	[31]
gold	-PEG-PFPE,	5 nm	3 and 30 μM	triblock PFPE-PEG-PFPE surfactant	–	W/FO + P	30 μm	flow focusing, PDMS	[53]
silica	-C18, -OH	100, 250 nm	10–20 wt%	PVA (in water)	pH	W/O + P/W	150 μm	flow focusing, glass capillary	[54]
silica	-C18, -OH	1.9 μm	3–50 $mg\,mL^{-1}$	–	–	O/O + P/W	200 μm	flow focusing, glass chip	[28]
various	various	20–250 nm and 10 μm	5.0 and 7.5 wt%	PVA (in water)	–	W/O + P/W	100–200 μm	flow focusing, glass capillary	[55]

[*] Not reported. [**] Size of aggregates. Abbreviations: PFPE: perfluorinated polyethers; PLS: protein–lipid solution; PNIPAm: poly(*N*-isopropylacrylamide) microgel; TMS: trimethylethoxysilane; T: temperature; FG: fluorinated gas; FO: fluorinated oil; G: gas; O: oil; P: particles; W: water.

the particles behave concomitantly as emulsifiers/foamers and catalysts.[6]

In PIC systems, the particle design becomes particularly challenging, since the presence of catalytic centers affects the surface properties (e.g., contact angle, roughness, surface charge). In parallel, the surface properties of the particles may impact their catalytic performance such as the accessibility of active centers, the co-adsorption and local segregation of reactants, as well as the effect of porosity. Engineering suitable particles is therefore an iterative and time-consuming process with no unique strategy existing in the literature so far. The catalytic performance of particle-stabilized dispersions is, however, (significantly) better than blank experiments, justifying the investment. As we will mention further in Section 6, a way to overcome the lack of prediction of particles for given applications and speed up their development is to use dedicated modeling tools to rationalize the particle assembly and the distribution of the immiscible reactants or gas and liquid in the vicinity of the active centers.

We summarize below key developments in L-L-S and G-L-S microreactors for chemo-, photo-, and biocatalysis using PAC and PIC approaches. Noteworthy, certain systems such as polymers may behave either as particles or molecules depending on the experimental conditions. In the case of ambiguity, we will still provide them as examples for a complete overview of possible options.

4.1. Acid–Base Chemocatalysis

Surface-active particles can generate L-L-S microreactors for C-C and C-O coupling reactions. Typical particles consist of organosilicas prepared by cocondensation of alkylsilane precursors, or grafting alkylsilanes on fumed/sol–gel silicas. Silica particles (150–300 nm) with C_8/C_{18} and $-C_3SO_3H$ groups are active and reusable for dodecanal acetalization with ethylene glycol (EG) towards biofuels in dodecanal-in-EG emulsions (Figure 2a).[62] Silica containing C_1 and $-PhSO_3H$ groups show $>87\%$ conversion for deacetalizing aromatic/aliphatic acetals in toluene-in-water emulsion (Figure 2b).[63] PS-grafted silica with $-SO_3H$ centers are efficient for glycerol etherification with dodecanol towards biosurfactants (Figure 2c).[64] By tuning the PS chain length and sulfonation degree, double emulsions are generated, enhancing glycerol-in-dodecanol diffusion.

Despite their versatility, silicas can hardly catalyze fat splitting or hydrolysis of triglycerides, even under emulsion.[65] In contrast, perfluorosulfonic superacid Aquivion® resins ($H_0 \approx 12$, 100–300 nm) promote the hydrolysis of glyceryl trilaurate (GTL) to lauric acid (LA) at 100 °C by stabilizing GTL-in-water emulsions (Figure 2d). A GTL conversion and LA yield of 46% and 34%, respectively, can be achieved with productivities of 18 and 40 $mmol\,(mol\,H^+)^{-1}$ As an alternative to emulsions, bijels reinforced with silica can afford full conversion and high robustness in the base hydrolysis of ethyl acetate using NaOH (Figure 2d).[66]

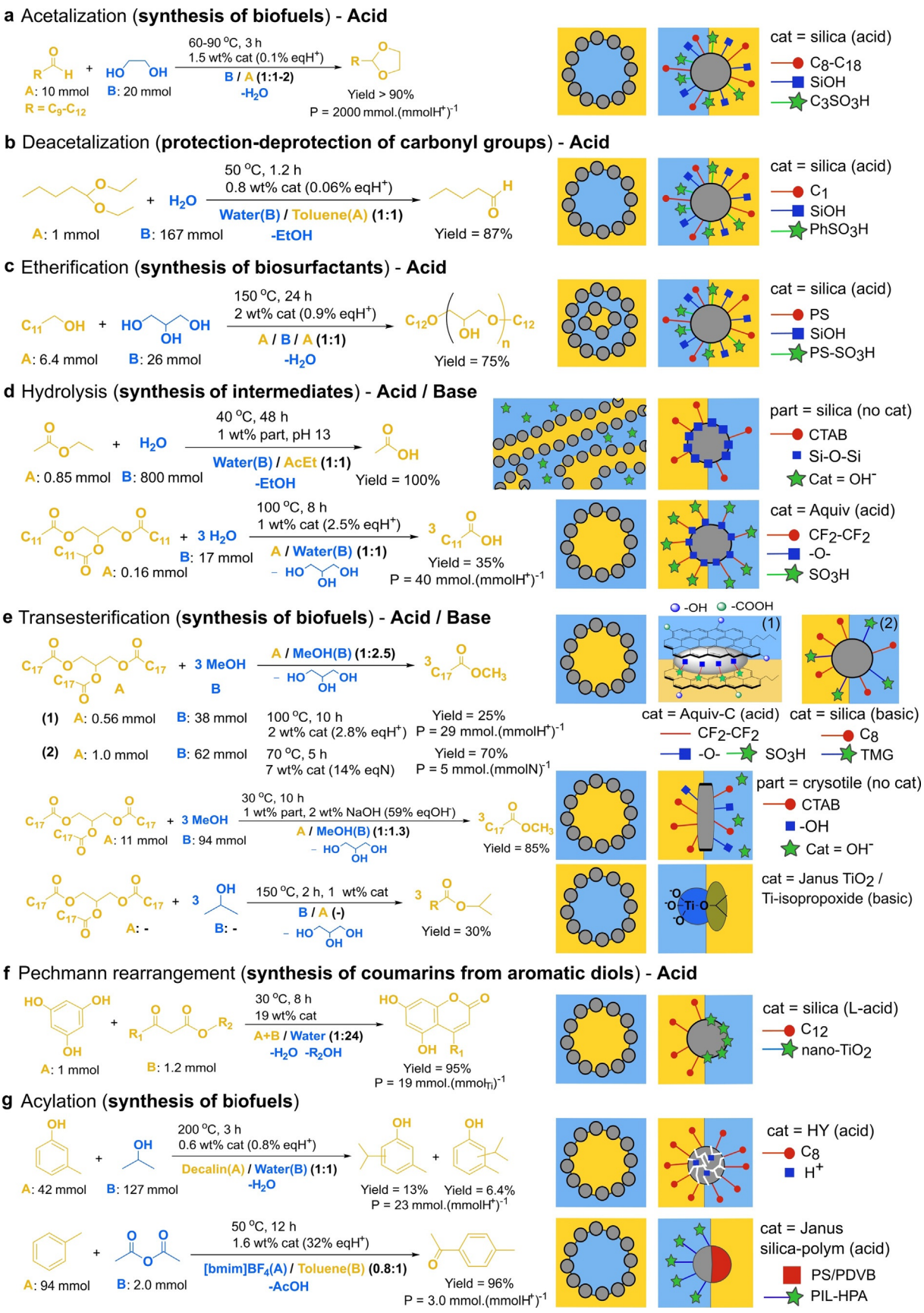

Figure 2. Particle-stabilized L-L microreactors for acid-base catalyzed reactions: a) Acetalization;[63] b) Deacetalization;[64] c) Etherification;[65] D) hydrolysis;[66,67] e) Transesterification;[68–71] f) Alkylation/acylation;[72,73] g) Pechmann rearrangement.[74]

Surface-active catalysts have been developed for biodiesel synthesis by transesterification of vegetable oils with methanol (MeOH) (Figure 2e). Aquivion®–carbon composites show high activity and reusability for GTO transesterification with MeOH at 100 °C.[67] The productivity after 10 h increases with the Aquivion® loading up to 29 mmol (mmol H^+)$^{-1}$ and correlates with the interfacial area. Soybean oil transesterification can also be conducted on basic silica modified with 1,1,3,3-tetramethylguanidine (TMG) and C_4–C_{16} chains with 67% conversion at 70 °C for 5 h by forming GTO-in-MeOH emulsions.[68] Magnetic hybrids based on chrysotile-CNTs exhibit 85% yield of biodiesel for soybean oil transesterification in oil-in-water emulsion with MeOH/KOH.[69] Finally, dendritic polymers derived from Ti-isopropoxide stabilize soybean oil-in-MeOH emulsions and catalyze the transesterification reaction with a yield of biodiesel up to 42% at 200 °C for 3 h.[70]

Surface-active acid catalysts have been engineered for alkylation/acylation reactions (Figure 2f). HY zeolites decorated with C_8 chains show high activity and reusability for *m*-cresol alkylation with 2-propanol in water-in-decalin emulsion.[71] The modified zeolite exhibits >35% *m*-cresol conversion at 200 °C for 5 h, whereas the parent zeolite only shows <10% conversion and is quickly deactivated. Poly(1-vinyl-3-ethylimidazolium bromide)-modified silica@PS/PDVB Janus particles incorporating $H_3PW_{12}O_{40}$ stabilize [BMIM]BF_4-in-toluene emulsions under flow and catalyze toluene acylation with acetic anhydride.[72] The catalyst can be reused six times.

L-L-S microreactors based on oil–particle aggregates have been developed for preparing coumarin derivatives via Pechmann condensation of phenol and β-ketoesters over Lewis acid catalysts based on nano-TiO_2 on C_{12}-sulfated silica (Figure 2g).[73] The high catalytic activity results from the formation of oil–particle aggregates in water, affording yields >90%.

4.2. Oxidation Reactions

L-L-S microreactors can be engineered for epoxidation reactions of alkenes with H_2O_2 (Figure 3a) Alkene epoxidation can be conducted over particles based on alkylammonium salts of polyoxometalates (i.e. [C_n]POM) stabilizing water-in-toluene emulsions (Figure 3a-1).[74] Besides, POMs can be either supported over surface-active silica microspheres (250–350 nm) modified with triamine and C_8 groups,[75] ionic copolymers,[76] and porous polyhedral oligomeric vinylsilsesquioxanes,[77] or encapsulated in a surfactant over silica.[78] In these examples, the catalysts possess a hydrophobic microenvironment surrounding POM, promoting the epoxidation of cyclic alkenes and allyl alcohols without stirring. POMs can also be hosted in the mesopores of silica nanospheres with zwitterionic and C_8 moieties.[79] By adjusting the surface properties, either oil-in-water or water-in-oil emulsions can be generated using a library of solvents, catalyzing the epoxidation of enols without stirring.

Surface-active titanosilicates based on TS-1 can be used to conduct alkene epoxidation in emulsion (Figure 3a-2). Hierarchical core/shell TS-1@silica/carbon particles have been prepared by self-assembly and nanocasting of titanosilicate crystals and surfactant-mediated mesosilica/resol precursors.[80] The particles stabilize 1-hexene-in-water emulsions, favoring 1-hexene epoxidation with TON = 15 mol (Ti-mol)$^{-1}$ at 60 °C for 1 h. Hollow TS-1 prepared by postsynthetic desilication with tetrapropylammonium hydroxide and silylation with hexamethyldisiloxane exhibits high activity for 1-hexene/cyclohexene epoxidation with H_2O_2 in water-in-oil emulsions.[81] The TOF increases with the degree of particle silanization with a maximum of 20.6 h^{-1} for 1-hexene.

L-L-S microreactors were developed for partial oxidation reactions (Figure 3b). Particles incorporating 2,2,6,6-tetramethylpiperidine-*N*-oxyl (TEMPO) are active for the Anelli oxidation of alcohols using NaClO/NaBr.[82] Crosslinked PS-covered Fe_3O_4 particles grafted with *N*-alkyl imidazole incorporating TEMPO and stabilizing water-in-CH_2Cl_2 emulsions can catalyze the oxidation of aromatic/aliphatic alcohols, enhancing the reaction rate due to the large interfacial area generated (Figure 3b-1).[83]

Surface-active particles hosting transition metal nanoparticles can also catalyze partial oxidation reactions. Hybrid catalysts based on Ru/CNT can perform the aerobic oxidation of alcohols with dissolved air/O_2 (Figure 3b-2).[84] The oxidation of benzyl alcohol to benzaldehyde is enhanced due to the genesis of water-in-oil emulsions. (Fe_2O_3-NiO_x)/Al_2O_3 particles functionalized with hexadecylphosphate acid stabilize water-in-toluene emulsions and catalyze toluene oxidation to benzaldehyde using dissolved O_2 as oxidant with 83% yield.[85] Au nanoparticles (10–15 nm) decorated with $PiBA_{20}$-*b*-$PDMS_{75}$-*b*-$PiBA_{20}$ copolymer (PiBA = polyisobornylacrylate, PDMS = polydimethyl-siloxane) can assemble at the water/$CHCl_3$ interface, catalyzing the oxidation of primary alkyl/aryl organosilanes towards poly(alkyl/arylhydrosiloxane)s.[86] Silica particles modified with C_8/polyamine groups can assemble at the gas–water interface, generating O_2 μ-bubbles that behave as G-L-S microreactors.[87] By incorporating Pd or Au nanoparticles, the particles become active for the aqueous oxidation of alcohols at the G-L interface with an enhanced activity compared to a conventional reactor. Also, O_2 μ-bubbles can be stabilized in water using a catalyst based on monodisperse Au nanoparticles embedded in $[PV_2Mo_{10}O_{40}]^{5-}$ assembled with 1,3,5-tris[(3-methylimidazolio)methyl]-2,4,6-trimethylbenzene tribromide by electrostatic interactions (Figure 3b-3).[88] The catalysts show high activity and reusability in the oxidation of aliphatic/aromatic alcohols into aldehydes/ketones with a yield up to 93% at 45 °C.

Particles based on TS-1 encapsulated on fibrous KCC silica grafted with C_8 chains stabilize water-in-benzene emulsions (Figure 3b-4).[89] The particles display an interfacial activity of 1.1 mol (Ti-mol)$^{-1}$ for benzene hydroxylation with excellent stability and good reusability. Ionic liquid functionalized Janus particles containing the Ti(salen) complex stabilize emulsions for sulfide/water systems (Figure 3b-5).[90] By optimizing the surface properties, the particles display high activity for asymmetric sulfoxidation reactions in water with >90% yield and >98% *ee*.

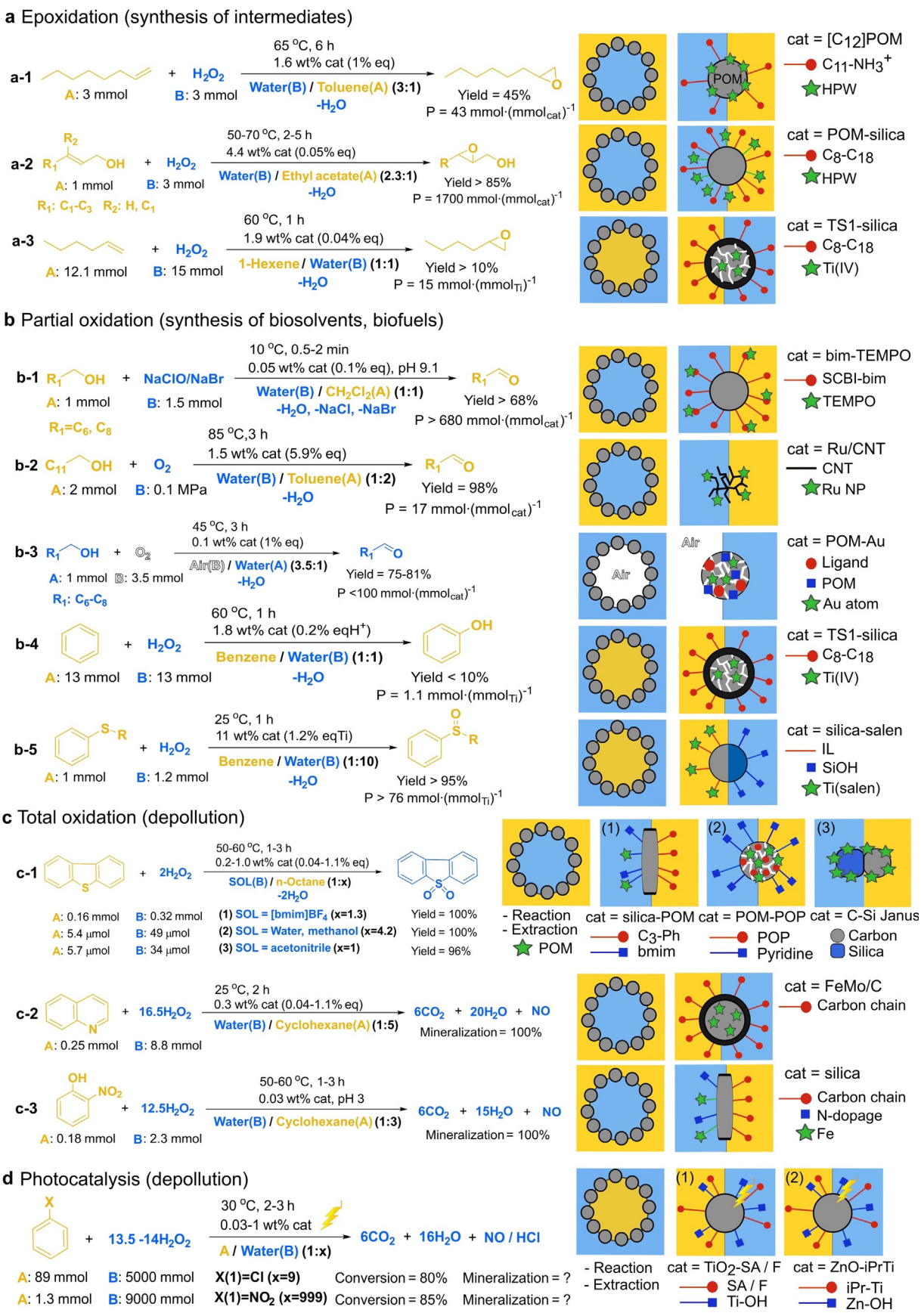

Figure 3. Particle-stabilized L-L-S microreactors for oxidation reactions: a) Epoxidation of olefins;[75,76,81] b) Partial oxidation of alcohols,[83,85,89] benzene hydroxylation,[90] and oxidation of sulfides[91] for synthesis; c) Partial/total oxidation[92–96] and photocatalytic oxidation[97,98] for depollution.

Specific developments have focused on oxidation reactions for depollution (Figure 3c). A first application encompasses emulsion desulfurization of sulfide compounds (e.g., dibenzothiophene) for marine diesel depollution, where the sulfide in the oil phase (usually *n*-octane) is oxidized to sulfone and further extracted to the polar phase (Figure 3c-1). Three main types of surface-active supported POM particles have been developed: 1) $[BMIM]_3PMo_{12}O_{40}$-type Janus nanosheets for $[bim]BF_4$-in-*n*-octane emulsions,[91] 2) POMs loaded on a hierarchical pyridine-based porous organic polymer for water–methanol-in-*n*-octane emulsions,[92] and 3) $PW_{12}O_{403-}$ supported over carbon-organosilica Janus particles for acetonitrile-in-*n*-octane emulsions.[93] In all cases, full S-removal is achieved at 50–60 °C within 1–3 h. The activity is much higher than that of conventional oxidative desulfurization without emulsion and stirring. The emulsions can be destabilized by centrifugation after reaction, and the particles can be reused five or six times. These systems can also be applied to the oxidation/extraction of N-containing pollutants such as quinoline. In particular, hybrid magnetic hybrids based on FeMo coated with CNTs stabilize water-in-cyclohexane emulsions and achieve quinoline mineralization with H_2O_2 at room temperature within 2 h (Figure 3c-2).[94] Janus N-doped CNTs stabilize oil-in-water emulsions simulating oily wastewaters. The CNTs allow 2-nitrophenol mineralization at 50 °C after 24 h with a stoichiometric amount of H_2O_2 (Figure 3c-3).[95]

Photocatalytic L-L-S microreactors have been developed based on semiconductor oxides for the degradation of poorly water-soluble pollutants (Figure 3d). TiO_2 particles modified with salicylic acid (SA) or fluorine,[96] as well as ZnO functionalized with (di(2-ethylhexyl)phosphate) isopropyl titanate,[97] can emulsify organic pollutants (e.g., monochlorobenzene, nitrobenzene) in water and achieve their complete photodegradation at room temperature, but with only partial mineralization. Ag_3PO_4@palygorskite clay particles stabilize oil-in-water emulsions and show efficient tetradecane photodegradation with 4.9 times higher removal efficiency than Ag_3PO_4 (not shown).[98] The high activity is attributed to the large surface area generated and to an efficient contact between Ag_3PO_4 and tetradecane, preventing agglomeration.

Examples of catalytic marbles applied to synthesis are scarce. Polyperoxides, which are valuable polymers, were prepared with good yield (>40%) by radical alternating copolymerization of 1,3-diene monomers with O_2 in 2-hydroxyethyl sorbate marbles stabilized by hydrophobic lycopodium particles, where O_2 permeates within the G-L interface.[99]

4.3. Reduction/Hydrogenation Reactions

L-L-S microreactors have been engineered for reduction reactions. Earlier examples focus on water-soluble $NaBH_4$ as the reducing reagent in water-in-oil and oil-in-water emulsions (Figure 4a). Snowman-like PDVB/PS-silica Janus particles loaded with Au nanoparticles on the silica side stabilize water-in-toluene emulsions with a 4–9-fold increase of *p*-nitroanisole (PNA) conversion compared to a two-phase system.[100] Dumbbell-shaped mesoporous carbon-organosilica Janus particles hosting Pt nanoparticles on the carbon side stabilize water-in-toluene emulsions and show a 3-fold activity increase for PNA reduction without stirring compared to Pt-loaded carbon spheres.[101] Janus nanosheets including Au nanoparticles on the hydrophilic side and phenyl groups on the hydrophobic side stabilize toluene-in-water emulsions.[102] The particles exhibit a 16-fold increase of *p*-nitroanisole (PNA) conversion compared to a two-phase system. Janus nanosheets with perpendicular mesoporous channels and two distinct surfaces display high interfacial activity and a highly accessible reaction interface.[103] By immobilizing Pd nanoparticles, the nanosheets exhibit a 4.5-fold activity increase for PNA reduction compared to Pd/SiO_2. Finally, surface-active Ag/GO (GO = graphene oxide) composites stabilize oil-in-water emulsions for a broad series of solvents at low pH.[104] In particular, double emulsions are generated for the benzyl chloride/water system, promoting 4-nitrophenol reduction owing to the large interfacial area generated.

Examples of L-L-S and G-L-S microreactors using H_2 as the reducing reagent have been recently reported (Figure 4b). Silica microspheres functionalized with triamine/C_8 groups and incorporating Pd nanoparticles show much higher activity than Pd/SiO_2 for styrene hydrogenation with dissolved H_2 due to the genesis of ethyl acetate in water emulsions.[105] The particles can be reused 36 times without apparent activity loss. Likewise, Pd/GO particles modified with methyltrimethoxysilane stabilize water-in-oil emulsions and promote the interfacial adsorption of cinnamaldehyde.[106] As a result, cinnamaldehyde hydrogenation is greatly promoted ($k = 0.121\ min^{-1}$) compared to the reaction over Pd/GO ($k = 0.021\ min^{-1}$), reaching 83% yield at 80 °C after 20 min. The particles can be reused four times without activity loss.

Surface-active CNT-supported Ni catalysts generate water-in-oil and oil-in-water emulsions based on dodecane.[107] The emulsion system is promising for furfural hydrogenation with 35% conversion and (≈80%) cyclopentanone selectivity at 200 °C and 20 MPa H_2 pressure for 1 h. G-L-S microreactors based on H_2/water foams that were engineered using silica particles modified with polyamine/C_8 groups exhibit 96% yield for 1,4-diol-2-butene hydrogenation, which is much higher than the value obtained in a three-phase reactor (35%).[87] A very high particle loading is required (7.5%) to stabilize the foams. Water marbles with hydrophobized silica combined with Ru/Al_2O_3 particles catalyze maleic acid hydrogenation to succinic acid at 70 °C and 20-bar H_2 atmosphere at the H_2–water interface with 50% conversion for 10 min without stirring.[108]

Specific developments have been reported for hydrodeoxygenation (HDO) reactions targeting the synthesis of biofuels (Figure 4c). Ru/CNT and Pd supported over carbon microspheres can catalyze vanillin HDO with >94% yield at 100–150 °C and 10 bar H_2 for 3 h by stabilizing water-in-decalin emulsions.[109] Janus silica particles with defined hydrophilic and silane-modified hydrophobic domains were impregnated with Pd either on the hydrophobic side or on the whole particles, stabilizing water-in-decalin emulsions.[110] In

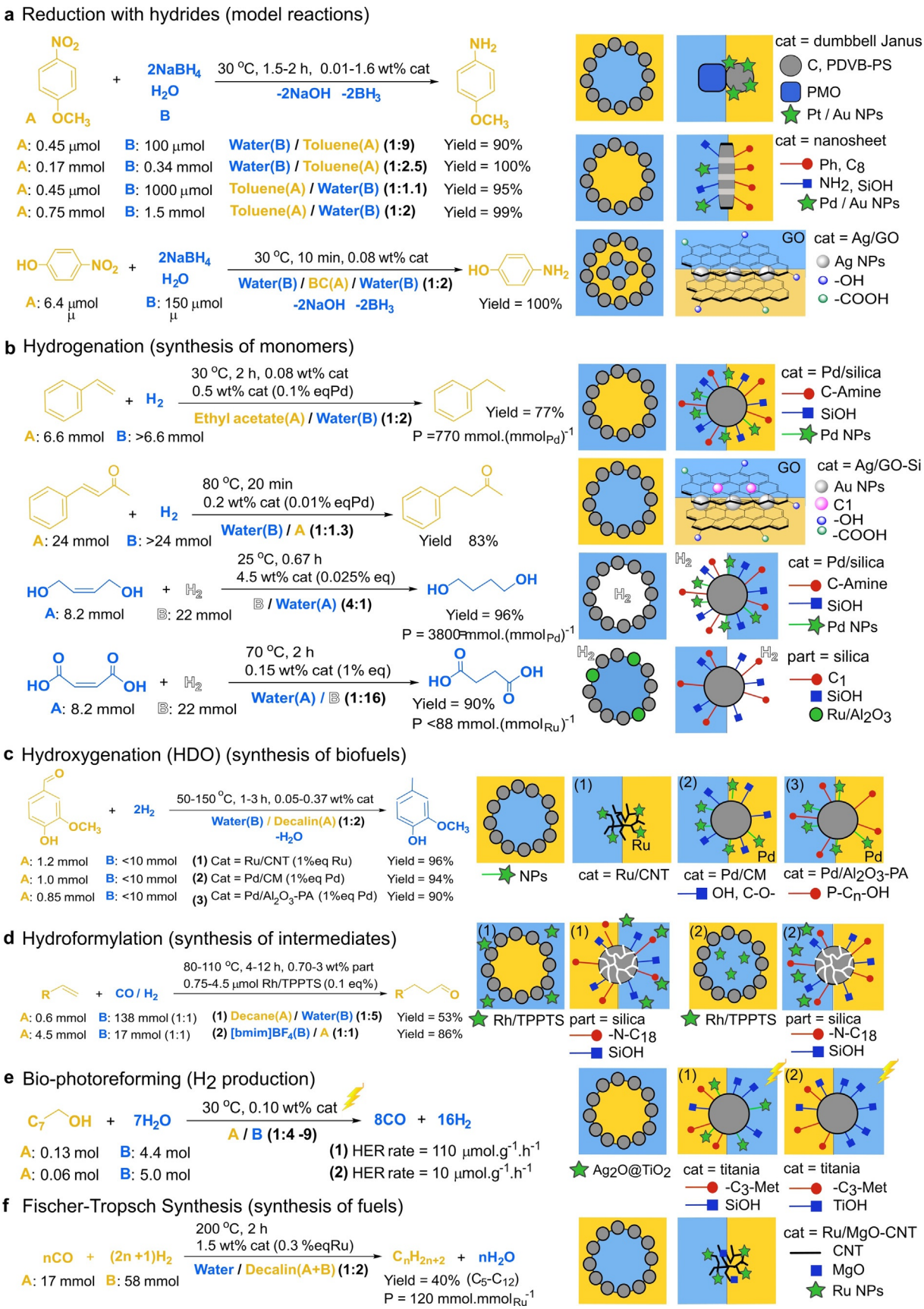

Figure 4. Particle-stabilized L-L-S and G-L-S microreactors for reduction/hydrogenation reactions: a) Reduction of *p*-nitroanisole/4-nitrophenol with aqueous $NaBH_4$;[101–105] b) Hydrogenation of activated double bonds;[88,106,107,109] c) Hydrodeoxygenation of vanillin;[110a,111,112] d) Hydroformylation of alkenes;[113,114] e) Bio-photoreforming of alcohols;[115,116] f) Fischer–Tropsch synthesis.[117a]

the former case, the rate constant for vanillin HDO is 2 orders of magnitude higher, pointing out an important role of the microenvironment on the catalytic performance. Pd/Al_2O_3 particles modified with organophosphonic acids and incorporating Brønsted acid centers can also stabilize water-in-decalin emulsions and catalyze vanillin HDO with a yield up to 90% at only 50°C for 1 h.[111] The activity enhancement depends on the hydrophobicity, impacting the selectivity and the emulsion morphology.

L-L-S microreactors for hydroformylation reactions have been recently reported by combining non-catalytic particles stabilizing emulsions and a water-soluble catalyst (Figure 4d). Mesoporous silica nanospheres modified with dimethyloctadecylammonium chains have been applied to 1-octene hydroformylation catalyzed by Rh-TPPTS.[112] Unlike the neat two-phase system, decane-in-water emulsions exhibit much higher TOF ($392\ h^{-1}$ vs. $56\ h^{-1}$) and aldehyde selectivity (79% vs. 46%) without stirring. The activity and aldehyde selectivity are much higher than the values measured on nonporous silica due to an enhanced diffusion of reactants within the mesopores. Dimethyl-octadecylammonium chains are regarded to favor Rh-TPPTS enrichment at the decane/water interface. The emulsion can be easily reused without obvious loss of activity. Surface-modified dendritic mesoporous silica nanospheres with (dimethyl-octadecyl[3-(trimethoxysilyl)propyl] ammonium groups stabilize $[BMIM]BF_4$-in-dodecene emulsions.[113] The emulsion system can catalyze 1-dodecene hydroformylation with Rh-TPPTS-sulfoxantphos with 94% chemoselectivity and $TOF = 413\ h^{-1}$. The pore size of the silica nanospheres impacts the diffusion of reactants to the catalytic centers. The catalysts can be reused five times without loss of either conversion or selectivity.

Two studies have been published targeting biool photoreforming for sustainable H_2 production in emulsion (Figure 4e). Surface-active Ag_2O-TiO_2/SiO_2 particles stabilize biooctanol-in-water emulsions and catalyze photoreforming H_2 production under solar light with a H_2 evolution rate (HER) of $110\ \mu mol\ g^{-1}\ h^{-1}$.[114] Cyclic H_2 production is improved by simple reemulsification. The reaction kinetics obeys a Langmuir–Hinshelwood type model. The particles can be recovered and reused without deactivation. TiO_2-based Janus particles with a half-surface modified with propylmethacrylate groups generate biooil-in-water emulsions.[115] The particles catalyze H_2 production by photoreforming of biooil substrates and water with an almost doubled H_2 yield compared to that on TiO_2 in two-phase system. The emulsification properties and catalytic stability exert a relevant effect on the cyclic stability.

Surface-active Ru/CNT-MgO and Ru/CNT-Al_2O_3 hybrids enable the formation of water-in-decalin emulsions and exert a positive effect on the activity and selectivity of Fischer–Tropsch synthesis, favoring a C_1/C_{5+} product balance (Figure 4f).[116] Unlike the reaction in a single-phase solvent, emulsions favor spontaneous separation of products driven by solubility differences, which affects mass-transfer-dependent secondary reactions.

Finally, very recently, Janus-type amphiphilic cellulose particles grafted with alkyl chains and incorporating palladium nanoparticles were prepared, which can stabilize oil-in-water emulsions.[117] The particles exhibit high activity in the Suzuki reaction at the water–oil interface at 80°C for 5 h in the presence of K_2CO_3. The catalyst can be recycled and reused for at least seven consecutive runs with a moderate decrease of activity.

4.4. Biocatalytic Reactions

Biocatalysis relies on the use of enzymes (typically lipases) and bacteria (Figure 5). Being molecules of biological origin, enzymes require aqueous media for proper conformation and related catalytic activity. Enzyme incorporation strategies involve either compartmentalization within emulsion droplets, or encapsulation in colloidal particles located at the oil/water interface (Figure 5a–c). Surface-active artificial enzyme particles have been prepared using peptide molecules, metal complexes, and DNAzymes as catalytic units.[118] The hybrid particles stabilize emulsions, enhancing the catalytic activity over that of native enzymes. Lipases can also be encapsulated by covalent coupling on aldehyde-modified Janus silica particles, enabling their location at the oil/water interface.[119] The specific activity of immobilized lipase is 6.5 and 1.4 times higher than that of free and liquid-core encapsulated lipases, respectively, for hexanoic acid esterification with 1-hexanol in water-in-heptane emulsion. The immobilized enzyme shows good stability and recyclability, retaining 75% of its activity after nine runs. Lipase-containing alginate gel particles with a coating of silanized titania nanoparticles have been used to generate water-in-oil emulsions for hexanoic acid esterification with 1-hexanol.[120] The hybrid particles exhibit high stability preserving 90% of the activity after ten runs. Immobilized lipases in mesoporous carbon nanospheres stabilize oil-in-water emulsions and exhibit much higher activity for phytosterol esterification than monophasic and biphasic systems, with 95% conversion after 90 min and a catalytic activity of $6.8\ mmol\ g^{-1}\ h^{-1}$.[121] This outstanding performance is attributed to enhanced lid opening of the lipase and rapid mass transfer of substrates to the oil/water interface. The particles show exceptional recyclability without apparent deactivation under harsh environments. The binary combination of hydrophobic silica particles and pH-responsive microgels hosting a lipase is a robust system that affords the formation of stable water-in-oil emulsions with high activity for 1-hexanoic acid esterification with 1-hexanol compared to a biphasic system without emulsion.[122] Finally, bijels have been reported as media to promote lipase-catalyzed hydrolysis of tributyrin in batch mode, showing a 4-fold increase of the reaction rate compared to a stirred biphasic medium.[123]

Examples of surface-functionalized bacteria as L-L-S microreactors have been reported in recent studies with potential applications in the biochemical industry (Figure 5d,e). Encapsulated bacterial whole cells (*A. faecalis*) within a mineral shell generate emulsions, enhancing the conversion of mandelic acid into (*R*,*S*)-mandelonitrile.[124] The mineral shell protects the entire cell from organic-solvent stress with reusability for 30 runs. Modified *E. coli* whole cells provided with lyase and hydrophobic silicone stabilize water-

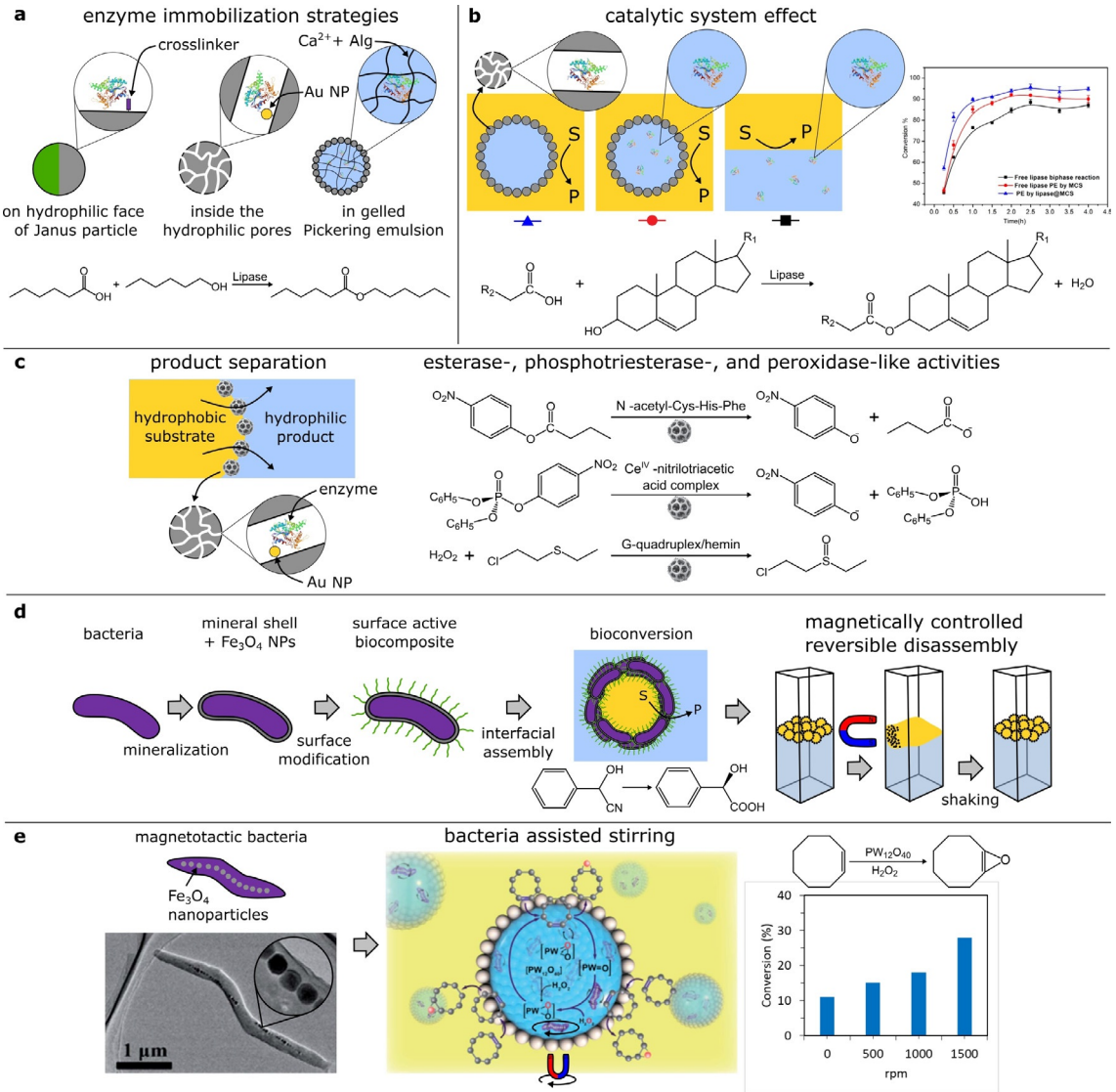

Figure 5. Particle-stabilized L-L microreactors for biocatalysis: a–c) Enzyme immobilization strategies, types of L-L microreactors based on enzymes and examples of reactions;[119–121] d) Preparation of surface-active bacteria, types of L-L microreactors based on bacteria and examples of reactions.[125–127]

in-oil emulsions and outperform the catalytic activity of emulsion-free benchmark systems for the stereoselective carboligation of benzaldehyde to (*R*)-benzoin.[125] Encapsulated magnetotactic bacteria in microdroplets have been used as nanoscale magnetic stirring bars to accelerate mass transfer under an external magnetic field.[126] Using cyclooctene epoxidation as model reaction, the reaction rate is enhanced 3 times compared to an emulsion, and 30 times compared to conventional stirred-driven biphasic systems under the same conditions.

5. Demulsification Methods

Separation of reaction products and recycling/reuse of catalytic particles requires destabilization of L-L-S and G-L-S microreactors (Figure 6, Table S2). However, the development of well-adapted technologies for reversible generation of L-L-S and G-L-S microreactors in industrial processes is still necessary. Coalescence of particle-stabilized dispersions can be achieved either by detaching particles from the interface, or by bridging bubbles/droplets via defects between the particles at deformed interfaces. Two types of methods can be distinguished: 1) use of an external force (Figure 6a-1) and 2) modification of the physicochemical properties of the system (Figure 6b-1).

Centrifugation is the most common and efficient method belonging to the first type that can be used to demulsify emulsions, including fluorinated solvents (Figure 6a-2).[127] Freeze–thaw treatment can coalesce emulsions by expelling particles from growing ice to the continuous phase.[128] A main shortcoming is that the dispersed phase must be frozen, whereas the continuous phase remains liquid, preventing the application of this method to foams, oil-in-water emulsions,

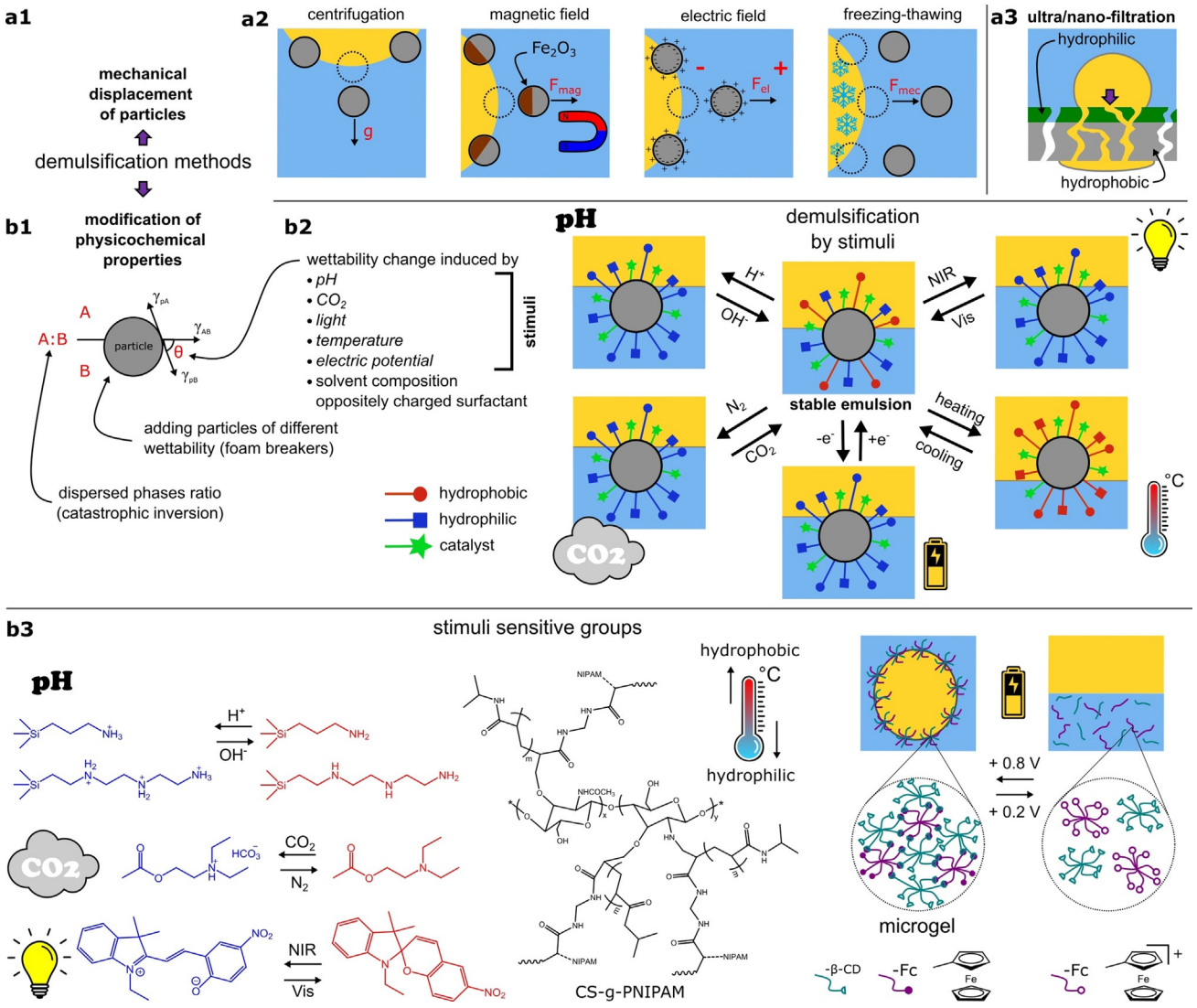

Figure 6. Demulsification methods. a) Mechanical particle detachment;[128,129,131,133,138a] b) Modification of physicochemical properties.[139,141a,145,147,148]

and marbles. Electrocoalescence is efficient for destabilizing oil-in-water emulsions with a threshold voltage decreasing with the particle size,[127] as well as for preparing liquid marbles.[129] Particle detachment can also be induced by a magnetic field on particles incorporating catalytic and magnetic (e.g., Fe_2O_3) nanoparticles, allowing the stabilization of reversible emulsions.[130] The merging of marbles stabilized by magnetic particles is also known:[131] two adjacent marbles are opened from the top by putting a strong magnet bar below the glass slide, and the exposed droplets coalesce to a larger marble. In the case of foams, two magnetically driven destabilization mechanisms are known: wet foams collapse due to bubble ejection from the particle matrix, while dry foam rupture occurs by film stretching.

Ultra- and nanofiltration membranes can promote oil/water and gas/water separation (Figure 6a-3). Different materials can be used, including polymers (e.g., cellulose fibers), ceramics, carbon nanotubes, and metal meshes.[132] Key to these materials is the engineering of superhydrophilic/superoleophobic ($\theta \approx 0°$) and superhydrophobic/superoleophilic ($\theta > 150°$) pores with affinity for either the polar or apolar phase.[133] The membranes can be either used to remove the continuous phase and preconcentrate droplets/bubbles, or to destabilize emulsions/foams and recover the particles. The first option is suitable for separating reaction products, enabling continuous processes incorporating L-L-S and G-L-S microreactors for recycling reactants/catalysts.[134] Recent advances cover organic solvent nanofiltration membranes for separating homogeneous catalysts/colloids, which can be applied to oleophilic particles.[135] Fouling can be avoided by surface modification such as coating with hydrophilic/oleophilic layers, grafting, particle deposition, and UV radiation.[136] A recent innovation involves Janus membranes with feed and permeate sides of opposite wettability or gradual pore wettability within the thickness, which is suitable for destabilizing surfactant-stabilized emulsions and foams.[137] However, to our knowledge, no application has been reported so far for particle-stabilized emulsions and

foams, which could provide significant progress for emulsion/foam destabilization.

Modification of the physicochemical properties can also favor particle detachment. In the case of emulsions, demulsification can be achieved by changing the ratio between the two phases, inducing catastrophic phase inversion (Figure 6b-1). Such effect can also switch marbles to foams by changing the air/water ratio.[138] An oppositely charged surfactant may be added for in situ hydrophobization of particles.[139] Also, particles with higher hydrophobicity can be added as a demulsifier with high efficiency even at very low loading (0.01 wt%).[140]

A change of the interfacial contact angle may be triggered by stimuli and used for demulsification (Figure 6b-2). pH-responsive particles can be designed by incorporating -NH_2, -SO_3H, and -COOH groups (Figure 6b-3). Silica nanospheres functionalized with C_8/polyamine groups and Pd nanoparticles can hydrogenate *p*-methylbenzaldehyde, isopropenylbenzene, butylmethacrylate, pentylacetylene, and styrene in ethyl acetate-in-water emulsions with recyclability for 15 runs.[141] The same particles can be applied for engineering pH-responsive foams.[87] Starch modified with *N*,*N*′-methylenebisacrylamide and Au nanoparticles generate ethyl acetate-in-water emulsions for PNA hydrogenation with reversible emulsification/demulsification for eight runs.[142] Tertiary amine containing microgels with Au particles can disperse organosilanes in oil-in-water emulsion and react with water for H_2 generation, exhibiting controllable demulsification/emulsification by bubbling CO_2/vacuuming.[143]

Temperature-responsive chitosan particles crosslinked with poly(*N*-isopropylacrylamide) (PNIPAM) enable reversible stabilization of oil-in-water emulsions, enhancing lipase performance for hydrolysis and esterification.[144] The oil phase containing products can be separated/reemulsified by tuning the temperature, allowing enzyme/microgel reutilization for six runs. UiO-66-PNIPAM hybrids with Pd nanoparticles stabilize toluene-in-water emulsions and promote chlorobenzene dechlorination.[145] The particles trigger emulsification at room temperature and demulsification at 45 °C, favoring product separation and particle reuse five times.

Electrochemically responsive microgels built from cyclodextrin-functionalized eight-arm poly(ethylene glycol) and ferrocene-modified counterparts can condition emulsion stability and be used to hydrolyze triacetin and resolve (*R*,*S*)-1-phenylethanol catalyzed by lipases.[146] Light-responsive particles based on interfacially active nanophosphors conjugated with photochromic sipropyrans show a hydrophilic–lipophilic conformational change in response to UV/Vis irradiation, resulting in emulsion inversion.[147] The particles show a reversible emulsion behavior and are efficient for the enantioselective hydrolysis of mandelonitirile (oil-soluble) to mandelic acid (water-soluble) using a model bacterium, *Alcaligenes faecalic* ATCC 8750, which locates in the water phase.

6. Advanced Concepts

6.1. Cascade Reactions

The field of cascade reactions is promising for engineering one-pot reactions targeting the synthesis of high-added-value chemicals. A first approach relies on the use of a single type of catalytic particle (alone or paired with a homogeneous catalyst) (Figure 7a–c). Earlier examples consist of SWCNT/silica hybrids stabilizing water-in-oil emulsions combined with an inorganic base (alternatively SWCNT/MgO was used), which catalyze the one-pot aldol condensation of 5-methylfurfural with acetone, followed by hydrogenation with concomitant phase transfer (Figure 7a).[148] Pd/graphitic carbon nitride (Pd/g-C_3N_4) composite can stabilize oil-in-water emulsions ensuring simultaneous catalysis of ammonia borane hydrolysis and hydrogenation of styrene into ethylbenzene by hydrogen from the first reaction (Figure 7b).[149] Janus particles based on a combined mesoporous silica nanorod (50–400 nm) and a mesoporous Fe_3O_4@C magnetic nanosphere (150 nm) can stabilize oil-in-water emulsions (Figure 7c).[150] By anchoring amine groups and Pt nanoparticles on the silica and carbon domains, respectively, the particles behave as bifunctional catalysts for the one-pot aldol condensation of benzaldehyde with acetaldehyde, followed by oxidation to cinnamic acid at 50 °C, with a TOF of 700 h^{-1}. UiO-66 grafted with poly[2-(diethylamino)ethyl methacrylate)] and incorporating Pd nanoparticles can stabilize toluene-in-water emulsions and catalyze the Knoevenagel condensation of nitrobenzaldehydes with malononitrile, followed by hydrogenation, with 95% overall yield at room temperature.[151] Enzyme–polymer conjugates based on poly(*N*-isopropylacrylamide) grown on glucose oxidase stabilize water-in-oil emulsions, leading to a 170-fold increase of activity in a four-step cascade reaction for the synthesis of cyclohexene epoxide from cyclohexene epoxidation.[152]

Interfacial one-pot reactions can be designed by the bottom-up interfacial self-assembly of two catalytic particles containing complementary hydrophilic/hydrophobic groups (tectons) driven by colloidal tectonics, generating water-in-toluene emulsions (Figure 7d).[153] Owing to attractive forces between tectons, small clusters are formed, becoming more and more amphiphilic. The internal surface remains highly porous and behaves as an open sponge with hydrophilic/hydrophobic regions where solvent or substrate molecules can be accommodated.[154] As an illustrative example, C_{12}-ammonium phosphotungstate particles and silica particles modified with C_{18}/C_3SO_3H groups self-assemble at the water/toluene interface by penetration of C_{18} chains of silica particles into the supramolecular porous structure of phosphotungstate particles. The emulsions serve in a non-nitric acid route for adipic acid synthesis from the one-pot oxidative cleavage of cyclohexene with aqueous H_2O_2.[155] Na_2HPO_4 and $[C_{12}]H_2PO_4$ condition the interlocking and self-assembly of the particles, enhancing the catalytic selectivity, especially for cyclooctene, with a yield of suberic acid up to 72%.

The combination of two surface-active hybrid catalysts based on zeolite NaX-MWCNT, containing Lewis acid centers, and sulfonated MWCNT, containing Brønsted acid

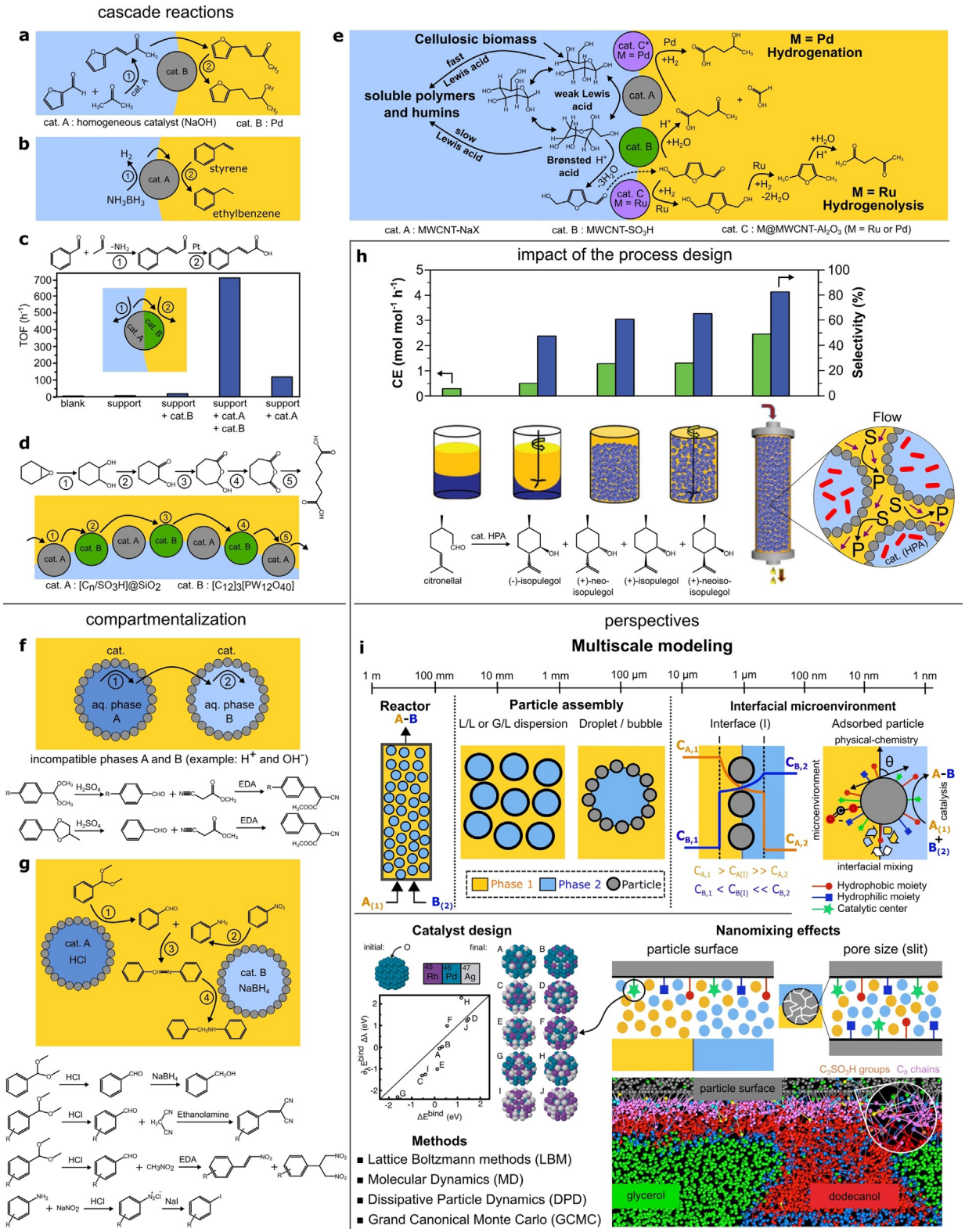

Figure 7. Advanced concepts and perspectives: a–e) Cascade reactions;[149a,150.151,154,157] f, g) Compartmentalized reactions;[158,159] h) Impact of the process design;[160] i, j) Multiscale modeling.

centers, can afford the isomerization of glucose to fructose, followed by its dehydration to hydroxymethylfurfural (HMF) with high conversion and HMF selectivity, by stabilizing water-in-decalin emulsions (Figure 7e).[156] The emulsion system favors continuous HMF separation into the organic phase. Through the incorporation of MWCNT-Al_2O_3 nanohybrids functionalized with Pd or Ru catalyst metal clusters into the system, HMF hydrolysis on Brønsted acid followed

by hydrogenation to γ-hydroxyvaleric acid or hydrogenolysis/hydration of HMF to 2,5-hexanedione over Pd or Ru, can be further achieved.

One-pot reactions can also be conducted in compartmentalized emulsion systems (Figure 7 f,g). Using layered emulsions stabilized by hydrophobic silica particles, catalytic cascades can be designed by compartmentalization of antagonistic catalysts or reagents. Examples include deacetalization–Knoevenagel cascades using a compartmentalized acid and base (Figure 7 f),[157] and deacetalization–reduction, deacetalization–Henry, and diazotization–iodization cascades using compartmentalized HCl and $NaBH_4$ (Figure 7 g).[158]

6.2. Impact on Process Design

Innovative developments have been reported for L-L reactions focusing on compartmentalized catalytic systems under flow. A continuous flow reactor using water droplets hosting a heteropolyacid exhibits 2–5-fold activity increase compared to a batch reactor for citronellal cyclization to (−)-isopulegol, along with excellent durability for two months (Figure 7 h).[159] Likewise, a continuous flow reactor with compartmentalized water droplets containing H_2SO_4, a heteropolyacid, or an enzyme can be immobilized in a packed column reactor in flowing organic phase.[160] The flow system exhibits 10-fold efficiency enhancement compared to a batch reactor and 2000-h durability on stream. Finally, methacrolein has been synthesized by the aldol condensation of propionaldehyde and formaldehyde by the Mannich reaction in a continuous flow process. The reactor is built with water-in-cyclohexane emulsions stabilized by hydrophobic silica particles and monoglyceride using diethanolamine acetate as the catalyst hosted in the water phase with an ionic liquid.[161] This continuous process exhibits a 1.25-fold increase of catalytic activity compared to a batch reactor, and the emulsion shows good stability in eight runs with neither ionic liquid leakage nor activity decrease. Besides, a continuous flow system based on a packed oil-in-water emulsion stabilized by aldehyde cellulose nanofibers decorated with Pd nanoparticles has been applied to 4-nitrophenol hydrogenation with dissolved H_2 for 55 h operation.[162] During the reaction, the H_2 flow creates favorable stirring for enhancing the contact between the reactants and metal nanoparticles, boosting the catalytic performance.

Overall, despite this progress, examples of continuous systems based on particle-stabilized foams and μ-bubbles have not been reported so far. Besides, implementation of oil foams into G-L catalytic systems could result in an outstanding progress for organic synthesis with potential impact in the cosmetic, oil, and manufacturing industries.[163] Owing to the low surface tension of organic solvents (typically ranging from 14 to 50 $mN\,m^{-1}$), the adsorption of common foam stabilizers at the gas–liquid interface is energetically unfavorable and requires stabilizers with low surface energy (e.g., fluorinated and polydimethylsiloxane surfactants), asphaltenes, or fatty acid crystals.[14b,18a,164] As a result, the generation of oil-based foams is much more challenging compared to aqueous foams.[164d,165]

6.3. Understanding the Reactivity

Modeling of L-L-S and G-L-S microreactors can provide valuable information for predicting their stability and rationalizing the particle location and rotation at the L-L and G-L interface, as well as the interfacial catalytic mechanisms (Figure 7 i). To this end, multiscale modeling affords an appropriate strategy, since multiphase emulsions are composed of microscale droplets, nanoscale particles, and reagent molecules.[166] In addition to other coarse-grained simulation techniques,[167] dissipative particle dynamics (DPD) represents a reliable method for predicting interfacial contact angles by simulating either the interfacial adsorption of one or multiple particles,[168] or the surface tension of reactants/liquids on particles.[169] Coalescence can be modeled by DPD including a reaction product,[158,170] and by molecular dynamics (MD) for describing the early stages of coalescence phenomena.[171] The dynamics of Pickering emulsion formation has been successfully modeled by lattice Boltzmann + MD simulations, encompassing the interfacial adsorption and rotation of single particles at short times, and their local reordering at longer times driven by capillary forces.[172]

Whereas the interfacial tension is not much influenced by the presence of large nanoparticles,[168b,171a] the local microenvironment can affect the catalytic activity/selectivity by conditioning the coadsorption, segregation, and diffusion of reactants near the active centers, as predicted by DPD and grand canonical Monte Carlo (GCMC) methods.[173] The interfacial porosity of microreactors is directly correlated to the size, shape, and polydispersity of colloidal particles. These properties can govern the three-phase contact line and line tension, as well as interparticle interactions, tuning the permeability of the particle layer and the access of reactants to the catalytic centers.[9c] The forces participating in the interparticle porosity can induce nanoscopic effects promoting the solubility between immiscible reactants.[170] Besides, enhanced solubility phenomena are known in mesoconfined liquids.[174] L-L and G-L interfaces can exhibit other nanoscopic phenomena with potential impact for catalysis, such as interfacial acidification/basification,[175] local solvation,[176] surface charge,[177] presence of diffusion barriers,[178] and molecule[179]/catalyst[180] orientation. Also, the spatial assembly of catalytic particles at the inner/outer interfacial layer of emulsion droplets can condition the catalytic selectivity, as recently illustrated for cinnamaldehyde hydrogenation.[181] Overall, these studies are useful for designing theoretical descriptors allowing fast discovery of L-L-S and G-L-S systems for target reactions, including new and unprecedented reactions (e.g., electrochemical reactions).[182]

7. Conclusions and Perspectives

In this Review, we have presented the most recent developments of liquid-liquid and gas-liquid dispersions stabilized by solid catalytic particles as microreactors for the synthesis of fine chemicals and depollution. These systems show high potential for reformulating already existing multiphasic reactors to render them more eco-efficient. Advanced

concepts comprise the engineering of one-pot reactions targeting the synthesis of added-value chemicals using either multisite catalytic particles, combinations of catalytic particles with different centers, self-assembly at the liquid–liquid or gas–liquid interface, or compartmentalized emulsion systems.

Innovative developments have been reported for liquid–liquid systems focusing on compartmentalized catalytic systems under flow. However, examples of continuous systems based on particle-stabilized foams and μ-bubbles have not been reported so far. Besides, implementation of oil foams into gas–liquid catalytic systems remains elusive and could lead to significant progress in the field.

The reported examples demonstrate the value of PIC systems and their potential application to processes of industrial interest. However, the selection of surface-active catalytic particles for PIC systems is still based on a trial-and-error approach and systematic methods for particle discovery are still missing. To sidestep this shortcoming, modeling liquid–liquid–solid and gas–liquid–solid microreactors could provide valuable information to predict their stability, rationalize the interfacial particle assembly, and elucidate the local microenvironment around the catalytic centers. To this aim, multiscale modeling methods are required, which can assist the design of theoretical descriptors, allowing fast discovery of liquid–liquid–solid and gas–liquid–solid systems for target reactions, including new and unprecedented reactions.

Last but not least, developing well-adapted tools for demulsification/defoaming and catalyst recovery/recycling still constitutes an unsolved challenge. Possible techniques based on external stimuli have been developed for demulsification/defoaming, but their implementation at industrial scale needs to be demonstrated. Nano- and ultrafiltration membranes can be used to either remove the continuous phase and preconcentrate droplets/bubbles, or destabilize emulsions/foams and recover the particles. The first option is suitable for separating reaction products, enabling continuous processes incorporating L-L-S and G-L-S microreactors for recycling reactants/catalysts. A recent innovation involves Janus membranes with feed and permeate sides of opposite wettability or gradual pore wettability within the thickness. Janus membranes have been applied to destabilize surfactant-stabilized emulsions and foams. However, to our knowledge, no application has been reported so far for particle-stabilized emulsions and foams, and this could provide significant progress for emulsion/foam destabilization.

Nomenclature

Abbreviations

$[BMIM]BF_4$	butyl-1-methyl-3-imidazolium tetrafluoroborate
CNT	carbon nanotube
DNAzyme	surface-active enzyme with catalytically active DNA
DPD	dissipative particle dynamics
EG	ethylene glycol
GCMC	grand canonical Monte Carlo
G-L	gas–liquid
G-L-S	gas–liquid–solid
GO	graphene oxide
GTL	glyceryl trilaurate
GTO	glyceryl trioleate
HDO	hydrodeoxygenation
HER	H_2 evolution rate
HMF	hydroxymethylfurfural
LA	lauric acid
L-L	liquid–liquid
MD	molecular dynamics
MWCNT	multiwalled carbon nanotube
PAC	Pickering assisted catalysis
PiBA	polyisobornylacrylate
PIC	Pickering interfacial catalysis
PDMS	polydimethylsiloxane
PNA	*p*-nitroanisole
PNIPAM	poly(*N*-isopropylacrylamide)
POM	polyoxometalate
PS	polystyrene
PDVB	polydivinyl benzene
SA	salicylic acid
SWCNT	single-walled carbon nanotube
TEMPO	2,2,6,6-tetramethylpiperidine-*N*-oxyl
TMG	1,1,3,3-tetramethylguanidine
TOF	turnover frequency [s^{-1}]
TON	turnover number
TPPTS	triphenylphosphine-3,3′3″-trisulfonate
TS	titanosilicate

Symbols

θ	contact angle
γ	surface tension
ΔG_d	minimum energy of particle desorption

Acknowledgements

This paper was funded by the French Agency of Research (ANR-17-ERC2-0030) and by the ERC grant Michelangelo (contract number #771586).

Conflict of Interest

The authors declare no conflict of interest.

Keywords: dispersions · interfacial catalysis · microreactors · multiphase reactions · sustainable chemistry

[1] a) P. A. Ramachandran, R. V. Chaudari, *Three-Phase Catalytic Reactors, Topics in Chemical Engineering*, *Vol. 2*, Gordon and Breach Science Publishers, Philadelphia, **1983**, Chapter 9; b) K-D. Henkel, *Reactor Types and their Industrial Applications*, Ullmann's Encyclopedia of Industrial Chemistry, *Vol. 31*, Wiley-VCH, Weinheim, **2012**, pp. 293–327.

[2] a) Y. T. Shah, *Gas-Liquid-Solid Reactor Design*, McGraw-Hill, NY, **1979**; b) P. Trambouze, J. P. Euzen, *Chemical Reactors:*

From Design to Operation, Editions Technip, Paris, **2004**; c) M. D. Dudukovic, Z. V. Kuzeljevic *Three-Phase Trickle-Bed Reactors*, Ullmann's Encyclopedia of Industrial Chemistry, *Vol. 31*, Wiley-VCH, Weinheim, **2013**, pp. 1 – 34.
[3] M. Pera-Titus, L. Leclercq, J.-M. Clacens, F. De Campo, V. Nardello-Rataj, *Angew. Chem. Int. Ed.* **2015**, *54*, 2006 – 2021; *Angew. Chem.* **2015**, *127*, 2028 – 2044.
[4] A. M. Bago Rodriguez, B. P. Binks, *Soft Matter* **2020**, *16*, 10221 – 10243.
[5] a) B. P. Binks, *Curr. Opin. Colloid Interface Sci.* **2002**, *7*, 21 – 41; b) B. P. Binks, *Langmuir* **2017**, *33*, 6947 – 6963; c) S. Arditty, C. P. Whitby, B. P. Binks, V. Schmitt, F. Leal-Calderon, *Eur. Phys. J. E* **2003**, *11*, 273 – 281.
[6] a) W. Drenckhan, *Angew. Chem. Int. Ed.* **2009**, *48*, 5245 – 5247; *Angew. Chem.* **2009**, *121*, 5347 – 5349; b) B. P. Binks, T. S. Horozov, *Angew. Chem. Int. Ed.* **2005**, *44*, 3722 – 3725; *Angew. Chem.* **2005**, *117*, 3788 – 3791; c) T. S. Horozov, *Curr. Opin. Colloid Interface Sci.* **2008**, *13*, 134 – 140; d) A. Stocco, R. Rio, B. P. Binks, D. Langevin, *Soft Matter* **2011**, *7*, 1260 – 1267.
[7] a) C. Casagrande, M. C. Veyssie, *C. R. Acad. Sci.* **1988**, *306*, 1423 – 1425; b) M. A. Fernandez-Rodriguez, M. A. Rodriguez-Valverde, M. A. Cabrerizo-Vilchez, R. Hidalgo-Alvarez, *Adv. Colloid Interface Sci.* **2016**, *233*, 240 – 254.
[8] S. Granick, S. Jiang, Q. Chen, *Phys. Today* **2009**, *62*, 68 – 69.
[9] a) J. H. Luo, M. X. Zeng, B. L. Peng, L. C. Zhang, P. M. Wang, L. P. He, D. L. Huang, Z. D. Cheng, *Angew. Chem. Int. Ed.* **2018**, *57*, 11752 – 11757; *Angew. Chem.* **2018**, *130*, 11926 – 11931; b) W. J. Xiang, S. L. Zhao, X. Y. Song, S. W. Fang, F. Wang, C. Zhong, Z. Y. Luo, *Phys. Chem. Chem. Phys.* **2017**, *19*, 7576 – 7586; c) D. Gonzalez Ortiz, C. Pochat-Bohatier, J. Cambedouzou, M. Bechelany, P. Miele, *Engineering* **2020**, *6*, 468 – 482.
[10] a) R. Aveyard, B. P. Binks, J. H. Clint, *Adv. Colloid Interface Sci.* **2003**, *100 – 102*, 503 – 546; b) B. Zhang, J. Wang, X. Zhang, *Langmuir* **2013**, *29*, 6652 – 6658.
[11] H. Wu, H. Watanabe, W. Ma, A. Fujimoto, T. Higuchi, K. Uesugi, A. Takeuchi, Y. Suzuki, H. Jinnai, A. Takahara, *Langmuir* **2013**, *29*, 14971 – 14975.
[12] S. S. Velankar, *Soft Matter* **2015**, *11*, 8393 – 8403.
[13] G. Sun, Y. Sheng, T. Ngai, *Soft Matter* **2016**, *12*, 542 – 545.
[14] a) S. E. Friberg, *Curr. Opin. Colloid Interface Sci.* **2010**, *15*, 359 – 364; b) A. L. Fameau, A. Saint-Jalmes, *Adv. Colloid Interface Sci.* **2017**, *247*, 454 – 464.
[15] a) G. Wang, K. Wang, C. Lu, Y. Wang, *Chem. J. Chin. Univ.* **2018**, *39*, 990 – 995; b) K. Wang, G. Wang, C. Lu, Y. Wang, *Micro Nano Lett.* **2018**, *13*, 397 – 402.
[16] a) L. Gao, T. J. McCarthy, *Langmuir* **2007**, *23*, 10445 – 10447; b) K. Shirato, M. Satoh, *Soft Matter* **2011**, *7*, 7191 – 7193.
[17] a) G. McHale, M. I. Newton, *Soft Matter* **2011**, *7*, 5473 – 5481; b) L. Forny, I. Pezron, K. Saleh, P. Guigon, L. Komunjer, *Powder Technol.* **2007**, *171*, 15 – 24; c) B. P. Binks, A. J. Johnson, J. A. Rodrigues, *Soft Matter* **2010**, *6*, 126 – 135.
[18] a) R. Murakami, A. Bismarck, *Adv. Funct. Mater.* **2010**, *20*, 732 – 737; b) B. P. Binks, A. T. Tyowua, *Soft Matter* **2013**, *9*, 834 – 845.
[19] T. N. Hunter, R. J. Pugh, G. V. Franks, G. J. Jameson, *Adv Colloid Interface Sci.* **2008**, *137*, 57 – 81.
[20] R. J. Pugh, *Adv. Colloid Interface Sci.* **2005**, *114 – 115*, 239 – 251.
[21] E. Dickinson, *An Introduction to food colloids*, Oxford University Press, Oxford, **1992**.
[22] a) M. Abkarian, A. B. Subramaniam, S. H. Kim, R. J. Larsen, S. M. Yang, H. A. Stone, *Phys. Rev. Lett.* **2007**, *99*, 188301; b) A. Stocco, W. Drenckhan, E. Rio, D. Langevin, B. P. Binks, *Soft Matter* **2009**, *5*, 2215 – 2222; c) R. Ettelaie, B. Murray, *J. Chem. Phys.* **2014**, *140*, 204713.
[23] D. E. Tambe, M. M. Sharma, *Adv. Colloid Interface Sci.* **1994**, *52*, 1 – 65.
[24] E. Dickinson, R. Ettelaie, T. Kostakis, B. S. Murray, *Langmuir* **2004**, *20*, 8517 – 8525.
[25] C. Albert, M. Beladjine, N. Tsapis, E. Fattal, F. Agnely, N. Huang, *J. Controlled Release* **2019**, *309*, 302 – 332.
[26] a) J. I. Park, Z. Nie, A. Kumachev, E. Kumacheva, *Soft Matter* **2010**, *6*, 630 – 634; b) J. Wan, H. A. Stone, *Langmuir* **2012**, *28*, 37 – 41; c) T. Brugarolas, F. Tu, D. Lee, *Soft Matter* **2013**, *9*, 9046 – 9058; d) A. J. Dixon, A. H. Dhanaliwala, J. L. Chen, J. A. Hossack, *Ultrasound Med. Biol.* **2013**, *39*, 1267 – 1276.
[27] J. I. Park, Z. Nie, A. Kumachev, A. I. Abdelrahman, B. P. Binks, H. A. Stone, E. A. Kumacheva, *Angew. Chem. Int. Ed.* **2009**, *48*, 5300 – 5304; *Angew. Chem.* **2009**, *121*, 5404 – 5408.
[28] G. Dockx, S. Geisel, D. G. Moore, E. Koos, A. R. Studart, J. Vermant, *Nat. Commun.* **2018**, *9*, 4763 – 4770.
[29] N. Yandrapalli, T. Robinson, M. Antonietti, B. Kumru, *Small* **2020**, *16*, 2001180.
[30] H. Chen, J. Li, W. Zhou, E. G. Pelan, S. D. Stoyanov, L. N. Arnaudov, H. A. Stone, *Langmuir* **2014**, *30*, 4262 – 4266.
[31] L. A. Chacon Orellana, J. Baret, *ChemSystemsChem* **2019**, *1*, 16 – 24.
[32] M. Seo, I. Gorelikov, R. Williams, N. Matsuura, *Langmuir* **2010**, *26*, 13855 – 13860.
[33] L. R. Arriaga, W. Drenckhan, A. Salonen, J. A. Rodrigues, R. Íñiguez-Palomares, E. Rio, D. Langevin, *Soft Matter* **2012**, *8*, 11085 – 11097.
[34] A. P. Kotula, S. L. Anna, *Soft Matter* **2012**, *8*, 10759 – 10772.
[35] E. Tumarkin, J. Park II, Z. Nie, E. Kumacheva, *Chem. Commun.* **2011**, *47*, 12712 – 12714.
[36] I. Liascukiene, G. Amselem, D. Z. Gunes, C. N. Baroud, *Soft Matter* **2018**, *14*, 992 – 1000.
[37] N. Taccoen, F. Lequeux, D. Z. Gunes, C. N. Baroud, *Phys. Rev. X* **2016**, *6*, 011010.
[38] A. B. Subramaniam, M. Abkarian, H. A. Stone, *Nat. Mater.* **2005**, *4*, 553 – 556.
[39] a) T. Brugarolas, B. J. Park, M. H. Lee, D. Lee, *Adv. Funct. Mater.* **2011**, *21*, 3924 – 3931; b) M. H. Lee, V. Prasad, D. Lee, *Langmuir* **2010**, *26*, 2227 – 2230.
[40] F. Zoueshtiagh, M. Baudoin, D. Guerrin, *Soft Matter* **2014**, *10*, 9403 – 9412.
[41] A. Gholamipour-Shirazi, M. S. Carvalho, J. O. Fossum, *Eur. Phys. J. Spec. Top.* **2016**, *225*, 757 – 765.
[42] Q. Y. Xu, M. Nakajima, B. P. Binks, *Colloids Surf. A* **2005**, *262*, 94 – 100.
[43] M. K. Mulligan, J. P. Rothstein, *Langmuir* **2011**, *27*, 9760 – 9768.
[44] X. Yao, Z. Liu, M. Ma, Y. Chao, Y. Gao, T. Kong, *Small* **2018**, *14*, 1802902.
[45] N. Abbasi, M. Navi, S. S. H. Tsai, *Langmuir* **2018**, *34*, 213 – 218.
[46] Z. Nie, J. Park II, W. Li, S. A. F. Bon, E. Kumacheva, *J. Am. Chem. Soc.* **2008**, *130*, 16508 – 16509.
[47] R. K. Shah, J. W. Kim, D. A. Weitz, *Langmuir* **2010**, *26*, 1561 – 1565.
[48] A. Schröder, J. Sprakel, K. Schroën, J. N. Spaen, C. C. Berton-Carabin, *J. Food Eng.* **2018**, *234*, 63 – 72.
[49] C. Priest, M. D. Reid, C. P. Whitby, *J. Colloid Interface Sci.* **2011**, *363*, 301 – 306.
[50] S. Fouilloux, F. Malloggi, J. Daillant, A. Thill, *Soft Matter* **2016**, *12*, 900 – 904.
[51] M. Pan, L. Rosenfeld, M. Kim, M. Xu, E. Lin, R. Derda, S. K. Y. Tang, *ACS Appl. Mater. Interfaces* **2014**, *6*, 21446 – 21453.
[52] L. A. Chacon Orellana, J. C. Baret, *J. Phys. D* **2017**, *50*, 39LT04.
[53] I. Platzman, J. W. Janiesch, J. P. Spatz, *J. Am. Chem. Soc.* **2013**, *135*, 3339 – 3342.
[54] J. S. Sander, A. R. Studart, *Langmuir* **2013**, *29*, 15168 – 15173.
[55] J. S. Sander, A. R. Studart, *Langmuir* **2011**, *27*, 3301 – 3307.

[56] a) N. Eshtiaghi, K. P. Hapgood, *Powder Technol.* **2012**, *223*, 65 – 76; b) T. Supakar, M. Moradiafrapoli, G. F. Christopher, J. O. Marston, *J. Colloid Interface Sci.* **2016**, *468*, 10 – 20.

[57] K. R. Sreejith, C. H. Ooi, J. Jin, D. V. Dao, N. T. Nguyen, *Rev. Sci. Instrum.* **2019**, *90*, 055102.

[58] P. M. Ireland, M. Noda, E. D. Jarrett, S. Fujii, Y. Nakamura, E. J. Wanless, G. B. Webber, *Powder Technol.* **2016**, *303*, 55 – 58.

[59] G. McHale, N. J. Shirtcliffe, M. I. Newton, F. B. Pyatt, S. H. Doerr, *Appl. Phys. Lett.* **2007**, *90*, 054110.

[60] W. Zhang, N. Srichan, A. F. Chrimes, M. Taylor, K. J. Berean, J. Z. Ou, T. Daeneke, A. P. O'Mullane, G. Bryant, K. Kalantar-Zadeh, *Sens. Actuators B* **2016**, *223*, 52 – 58.

[61] L. Forny, K. Saleh, I. Pezron, L. Komunjer, P. Guigon, *Powder Technol.* **2009**, *189*, 263 – 269.

[62] W.-J. Zhou, L. Fang, Z. Y. Fan, B. Albela, L. Bonneviot, F. De Campo, M. Pera-Titus, J.-M. Clacens, *J. Am. Chem. Soc.* **2014**, *136*, 4869 – 4872.

[63] S. Chen, F. Zhang, M. Yang, X. Li, H. Liang, Y. Qiao, D. Liu, W. Fan, *Appl. Catal. A* **2016**, *513*, 47 – 52.

[64] H. Shi, Z.-Y. Fan, V. Ponsinet, R. Sellier, H.-L. Liu, M. Pera-Titus, J.-M. Clacens, *ChemCatChem* **2015**, *7*, 3229 – 3233.

[65] H. Shi, Z.-Y. Fan, B. Hong, M. Pera-Titus, *ChemSusChem* **2017**, *10*, 3363 – 3367.

[66] G. Di Vitantonio, T. Wang, M. F. Haase, K. J. Stebe, D. Lee, *ACS Nano* **2019**, *13*, 26 – 31.

[67] W. Peng, P. Hao, J. Luo, B. Peng, X. Han, H. L. Liu, *Ind. Eng. Chem. Res.* **2020**, *59*, 4273 – 4280.

[68] S. Zhang, B. Hong, Z.-Y. Fan, J. Lu, Y. Xu, M. Pera-Titus, *ACS Appl. Mater. Interfaces* **2018**, *10*, 26795 – 26804.

[69] A. P. C. Teixeira, A. D. Purceno, A. S. Barros, B. R. S. Lemos, J. D. Ardisson, W. A. A. Macedo, E. C. O. Nassor, C. C. Amorim, F. C. C. Moura, M. G. Hernández-Terrones, F. M. Portela, R. M. Lago, *Catal. Today* **2012**, *190*, 133 – 143.

[70] G. Nawaratna, S. D. Fernando, S. Adhikari, *Energy Fuels* **2010**, *24*, 4123 – 4129.

[71] P. A. Zapata, J. Faria, M. P. Ruiz, R. E. Jentoft, D. E. Resasco, *J. Am. Chem. Soc.* **2012**, *134*, 8570 – 8578.

[72] X. Tang, Y. Hou, Q. B. Meng, G. Zhang, F. Liang, X.-M. Song, *Colloids Surf. A* **2019**, *570*, 191 – 198.

[73] A. Khalafi-Nezhad, S. M. Haghighi, F. Panahi, *ACS Sustainable Chem. Eng.* **2013**, *1*, 1015 – 1023.

[74] L. Leclercq, A. Mouret, A. Proust, V. Schmitt, P. Bauduin, J.-M. Aubry, V. Nardello-Rataj, *Chem. Eur. J.* **2012**, *18*, 14352 – 14358.

[75] W.-J. Zhang, L. Fu, H. Yang, *ChemSusChem* **2014**, *7*, 391 – 396.

[76] Y. Leng, J. Wu, P. Jiang, J. Wang, *Catal. Sci. Technol.* **2014**, *4*, 1293 – 1300.

[77] Y. Leng, J. Zhao, P. Jiang, J. Wang, *RSC Adv.* **2015**, *5*, 17709 – 17715.

[78] W. Qi, Y. Z. Wang, W. Li, L. X. Wu, *Chem. Eur. J.* **2010**, *16*, 1068 – 1078.

[79] F. Xue, Y. Zhang, F. Zhang, X. Ren, H. Yang, *ACS Appl. Mater. Interfaces* **2017**, *9*, 8403 – 8412.

[80] Y. Ding, H. Xu, H. Wu, M. He, P. Wu, *Chem. Commun.* **2018**, *54*, 7932 – 7935.

[81] G. Lv, F. Wang, X. Zhang, B. P. Binks, *Langmuir* **2018**, *34*, 302 – 310.

[82] J. Tang, Q. Zhang, K. Hu, P. Zhang, J. Wang, *J. Catal.* **2017**, *353*, 192 – 198.

[83] L. Feng, J. Wang, L. Chen, M. Lu, Z. Zheng, R. Jing, H. Chen, X. Shen, *ChemCatChem* **2015**, *7*, 616 – 624.

[84] X. Yang, X. Wang, J. Qiu, *Appl. Catal. A* **2010**, *382*, 131 – 137.

[85] C. Deng, M. Xu, Z. Dong, L. Li, J. Yang, X. Guo, L. Peng, N. Xue, Y. Zhu, W. Ding, *Chin. J. Catal.* **2020**, *41*, 341 – 349.

[86] R. Shankar, B. Jangir, A. Sharma, *RSC Adv.* **2017**, *7*, 344 – 351.

[87] J. Huang, F. Cheng, B. P. Binks, H. Yang, *J. Am. Chem. Soc.* **2015**, *137*, 15015 – 15025.

[88] Z. Huang, F. Li, B. Chen, G. Yuan, *Green Chem.* **2015**, *17*, 2325 – 2329.

[89] Y. Yang, W.-J. Zhou, A. Liebens, J.-M. Clacens, M. Pera-Titus, P. Wu, *J. Phys. Chem. C* **2015**, *119*, 25377 – 25384.

[90] M. Zhang, Z. Tang, W. Fu, W. Wang, R. Tan, D. Yin, *Chem. Commun.* **2019**, *55*, 592 – 595.

[91] L. Xia, H. Zhang, Z. Wei, Y. Jiang, L. Zhang, J. Zhao, J. Zhang, L. Dong, E. Li, L. Ruhlmann, Q. Zhang, *Chem. Eur. J.* **2017**, *23*, 1920 – 1929.

[92] R. Xia, W. Lv, K. Zhao, S. Ma, J. Hu, H. Wang, H. L. Liu, *Langmuir* **2019**, *35*, 3963 – 3971.

[93] S.-Y. Dou, R. Wang, *Chem. Eng. J.* **2019**, *369*, 64 – 76.

[94] R. V. Mambrini, C. Z. Maia, J. D. Ardisson, P. P. de Souza, F. C. C. Moura, *New J. Chem.* **2017**, *41*, 142 – 150.

[95] J. L. Diaz de Tuesta, B. F. Machado, P. Serp, A. M. T. Silva, J. L. Faria, H. T. Gomes, *Catal. Today* **2020**, *356*, 205 – 215.

[96] a) N. Fessi, M. F. Nsib, Y. Chevalier, C. Guillard, F. Dappozze, A. Houas, L. Palmisano, F. Parrino, *Langmuir* **2019**, *35*, 2129 – 2136; b) N. Fessi, M. F. Nsib, Y. Chevalier, C. Guillard, F. Dappozze, A. Houas, L. Palmisano, F. Parrino, *Langmuir* **2020**, *36*, 13545 – 13554.

[97] S. Zhang, L. Lei, Y. Liu, Q. Zhang, *Chin. J. Chem. Eng.* **2017**, *25*, 223 – 231.

[98] C. Han, Y. Li, W. Wang, Y. Hou, D. Chen, *Sci. Total Environ.* **2020**, *704*, 135356.

[99] E. Sato, M. Yuri, S. Fujii, T. Nishiyama, Y. Nakamura, H. Horibe, *Chem. Commun.* **2015**, *51*, 17241 – 17244.

[100] Y. Liu, J. Hu, X. Yu, X. Xu, Y. Gao, H. Li, F. Liang, *J. Colloid Interface Sci.* **2017**, *490*, 357 – 364.

[101] T. Yang, L. Wei, L. Jing, J. Liang, X. Zhang, M. Tang, M. J. Monteiro, Y. I. Chen, Y. Wang, S. Gu, D. Zhao, H. Yang, J. Liu, G. Q. M. Lu, *Angew. Chem. Int. Ed.* **2017**, *56*, 8459 – 8463; *Angew. Chem.* **2017**, *129*, 8579 – 8583.

[102] X. Xu, Y. Liu, Y. Gao, H. Li, *Colloids Surf. A* **2017**, *529*, 613 – 620.

[103] S. Yan, H. Zou, S. Chen, N. Xue, H. Yang, *Chem. Commun.* **2018**, *54*, 10455 – 10458.

[104] Y. He, F. Wu, X. Sun, R. Li, Y. Guo, C. Li, L. Zhang, F. Xing, W. Wang, J. Gao, *ACS Appl. Mater. Interfaces* **2013**, *5*, 4843 – 4855.

[105] H. Yang, T. Zhou, W. Zhang, *Angew. Chem. Int. Ed.* **2013**, *52*, 7455 – 7459; *Angew. Chem.* **2013**, *125*, 7603 – 7607.

[106] B. Xue, T. Xu, D. Li, J. Xu, Y. Li, F. Wang, J. Zhu, *J. Catal. Sci. Technol.* **2020**, *10*, 1096 – 1105.

[107] C. Herrera, D. Fuentealba, I. T. Ghampson, C. Sepulveda, J. L. Garcia-Fierro, R. I. Canale, N. Escalona, *Catal. Commun.* **2020**, *144*, 106092.

[108] B. O. Carter, D. J. Adams, A. I. Cooper, *Green Chem.* **2010**, *12*, 783 – 785.

[109] a) X. Yang, Y. Liang, Y. Cheng, W. Song, X. Wang, Z. Wang, J. Qiu, *Catal. Commun.* **2014**, *47*, 28 – 31; b) Z. Zhu, H. Tan, J. Wang, S. Yu, K. Zhou, *Green Chem.* **2014**, *16*, 2636 – 2643.

[110] B. Greydanus, D. K. Schwartz, J. W. Medlin, *ACS Appl. Mater. Interfaces* **2020**, *12*, 2338 – 2345.

[111] P. Hao, D. K. Schwartz, W. J. Medlin, *ACS Catal.* **2018**, *8*, 11165 – 11173.

[112] Y. Zhao, X. Zhang, J. Sanjeevi, Q. Yang, *J. Catal.* **2016**, *334*, 52 – 59.

[113] L. Tao, M. Zhong, J. Chen, S. Jayakumar, L. Liu, H. Li, Q. Yang, *Green Chem.* **2018**, *20*, 188 – 196.

[114] C. Wang, E. Bu, Y. Chen, Z. Cheng, J. Zhang, R. Shu, Q. Song, *Renewable Energy* **2019**, *134*, 113 – 124.

[115] E. Bu, Y. Chen, C. Wang, Z. Cheng, X. Luo, R. Shu, J. Zhang, M. Liao, Z. Jiang, Q. Song, *Chem. Eng. J.* **2019**, *370*, 646 – 657.

[116] a) D. Shi, J. Faria, T. N. Pham, D. E. Resasco, *ACS Catal.* **2014**, *4*, 1944 – 1952; b) D. Shi, J. A. Faria, A. A. Rownaghi, R. L. Huhnke, D. E. Resasco, *Energy Fuels* **2013**, *27*, 6118 – 6124.

[117] D.-D. Li, J.-Z. Jiang, C. Cai, *Chem. Commun.* **2020**, *56*, 9396 – 9399.

[118] Z. Chen, C. Zhao, E. Ju, H. Ji, J. Ren, B. P. Binks, X. Qu, *Adv. Mater.* **2016**, *28*, 1682 – 1688.

[119] J. Wang, R. Huang, W. Qi, R. Su, Z. He, *Langmuir* **2017**, *33*, 12317 – 12325.

[120] X. Yang, Y. Wang, R. Bai, H. Ma, W. Wang, H. Sun, Y. Dong, F. Qu, Q. Tang, T. Guo, B. P. Binks, T. Meng, *Green Chem.* **2019**, *21*, 2229 – 2233.

[121] Z. Dong, Z. Liu, J. Shi, H. Tang, X. Xiang, F. Huang, M. Zheng, *ACS Sustainable Chem. Eng.* **2019**, *7*, 7619 – 7629.

[122] H. Jiang, L. Liu, Y. Li, S. Yin, T. Ngai, *ACS Appl. Mater. Interfaces* **2020**, *12*, 4989 – 4997.

[123] S. Cha, H. G. Lim, M. F. Haase, K. J. Stebe, G. Y. Jung, D. Lee, *Sci. Rep.* **2019**, *9*, 6363.

[124] Z. Chen, H. Ji, C. Zhao, E. Ju, J. Ren, X. Qu, *Angew. Chem. Int. Ed.* **2015**, *54*, 4904 – 4908; *Angew. Chem.* **2015**, *127*, 4986 – 4990.

[125] R. Röllig, C. Plikat, M. B. Ansorge-Schumacher, *Angew. Chem. Int. Ed.* **2019**, *58*, 12960 – 12963; *Angew. Chem.* **2019**, *131*, 13094 – 13097.

[126] X. Zhou, C. Chen, C. Cao, T. Song, H. Yang, W. Song, *Chem. Sci.* **2018**, *9*, 2575 – 2580.

[127] a) M. Pan, F. Lyu, S. K. Y. Tang, *Methods* **2017**, *9*, 4622 – 4629; b) A. M. Bago Rodriguez, L. Schober, A. Hinzmann, H. Gröger, B. P. Binks, *Angew. Chem. Int. Ed.* **2021**, *60*, 1450 – 1457; *Angew. Chem.* **2021**, *133*, 1470 – 1477.

[128] S. Deville, *Science* **2018**, *360*, 303 – 306.

[129] Z. Liu, X. Fu, B. P. Binks, H. C. Shum, *Soft Matter* **2017**, *13*, 119 – 124.

[130] J. Cho, J. Cho, H. Kim, M. Lim, H. Jo, H. Kim, S.-J. Min, H. Rhee, J. W. Kim, *Green Chem.* **2018**, *20*, 2840 – 2844.

[131] Y. Zhao, J. Fang, H. Wang, X. Wang, T. Lin, *Adv. Mater.* **2010**, *22*, 707 – 710.

[132] N. Ali, M. Bilal, A. Khan, F. Ali, H. M. N. Iqbal, *TrAC Trends Anal. Chem.* **2020**, *127*, 115902.

[133] P. Marchetti, M. F. Jimenez Solomon, G. Szekely, A. G. Livingston, *Chem. Rev.* **2014**, *114*, 10735 – 10806.

[134] a) T. Skale, L. Hohl, M. Kraume, A. Drews, *J. Membr. Sci.* **2017**, *535*, 1 – 9; b) A. Heyse, C. Plikat, M. Grün, S. Delaval, M. Ansorge-Schumacher, A. Drews, *Process Biochem.* **2018**, *72*, 86 – 95; c) A. Heyse, C. Plikat, M. Ansorge-Schumacher, A. Drews, *Catal. Today* **2019**, *331*, 60 – 67; d) M. V. Kempin, M. Kraume, A. Drew, *J. Colloid Interface Sci.* **2020**, *573*, 135 – 149; e) S. Stock, A. Schlander, M. Kempin, R. Geisler, D. Stehl, K. Spanheimer, N. Hondow, S. Micklethwaite, A. Weber, R. Schomacker, A. Drews, M. Gallei, R. von Klitzing, *Phys. Chem. Chem. Phys.* **2021**, *23*, 2355 – 2367.

[135] a) S. Roy Chowdhury, P. T. Witte, D. H. A. Blank, P. L. Alsters, J. E. ten Elshof, *Chem. Eur. J.* **2006**, *12*, 3061 – 3066; b) A. S. Räder, I. C. Tessaro, L. D. Ferreira Marczak, *Can. J. Chem. Eng.* **2011**, *89*, 139 – 147; c) T. Li, A. W.-K. Law, M. Cetin, A. G. Fane, *J. Membr. Sci.* **2013**, *427*, 230 – 239.

[136] a) J. Ayyavoo, T. P. N. Nguyen, B.-N. Jun, I.-C. Kim, *Colloids Surf. A* **2016**, *506*, 190 – 201; b) R. Zhang, Y. Liu, M. He, Y. Su, X. Zhao, M. Elimelech, Z. Jiang, *Chem. Soc. Rev.* **2016**, *45*, 5888 – 5924.

[137] a) J. Yang, H.-N. Lo, Z.-X. Chen, A. He, Q.-Z. Zhong, Z.-K. Xu, *J. Mater. Chem. A* **2019**, *7*, 7907 – 7917; b) H.-C. Yang, J. Hou, V. Chen, Z.-K. Xu, *Angew. Chem. Int. Ed.* **2016**, *55*, 13398 – 13407; *Angew. Chem.* **2016**, *128*, 13596 – 13605; c) C. Pei, Y. Peng, Y. Zhang, D. Tian, K. Liu, L. Jiang, *ACS Nano* **2018**, *12*, 5489 – 5494; d) H. Zhou, Z. Guo, *J. Mater. Chem. A* **2019**, *7*, 12921 – 12950.

[138] B. P. Binks, R. Murakami, *Nat. Mater.* **2006**, *5*, 865 – 869.

[139] Y. Zhu, X. Pei, J. Jiang, Z. Cui, B. P. Binks, *Langmuir* **2015**, *31*, 12937 – 12943.

[140] C. Griffith, H. Daigle, *J. Colloid Interface Sci.* **2019**, *547*, 117 – 126.

[141] a) J. Huang, H. Yang, *Chem. Commun.* **2015**, *51*, 7333 – 7336; b) Y. Hao, Y. Liu, R. Yang, X. Zhang, J. Liu, H. Yang, *Chin. Chem. Lett.* **2018**, *29*, 778 – 782.

[142] L. Qi, Z. Luo, X. Lu, *Green Chem.* **2018**, *20*, 1538 – 1550.

[143] Y. Zhang, H. Zhang, P. Liu, H. Sun, B.-G. Li, W.-J. Wang, *ACS Sustainable Chem. Eng.* **2019**, *7*, 7768 – 7776.

[144] Y. Wang, L. Zhu, H. Zhang, H. Huang, L. Jiang, *Carbohydr. Polym.* **2020**, *241*, 116373.

[145] B.-J. Yao, Q.-J. Fu, A.-X. Li, X.-M. Zhang, Y.-A. Li, Y.-B. Dong, *Green Chem.* **2019**, *21*, 1625 – 1634.

[146] L. Peng, A. Feng, S. Liu, M. Huo, T. Fang, K. Wang, Y. Wei, X. Wang, J. Yuan, *ACS Appl. Mater. Interfaces* **2016**, *8*, 29203 – 29207.

[147] Z. Chen, L. Zhou, W. Bing, Z. Zhang, Z. Li, J. Ren, X. Qu, *J. Am. Chem. Soc.* **2014**, *136*, 7498 – 7504.

[148] a) S. Crossley, J. Faria, M. Shen, D. E. Resasco, *Science* **2010**, *327*, 68 – 72; b) P. A. Zapata, J. Faria, M. P. Ruiz, D. E. Resasco, *Top. Catal.* **2012**, *55*, 38 – 52.

[149] C. Han, P. Meng, E. R. Waclawik, C. Zhang, X.-H. Li, H. Yang, M. Antonietti, J. Xu, *Angew. Chem. Int. Ed.* **2018**, *57*, 14857 – 14861; *Angew. Chem.* **2018**, *130*, 15073 – 15077.

[150] T. Zhao, X. Zhu, C.-T. Hung, P. Wang, A. Elzatahry, A. A. Al-Khalaf, W. N. Hozzein, F. Zhang, X. Li, D. Zhao, *J. Am. Chem. Soc.* **2018**, *140*, 10009 – 10015.

[151] W.-L. Jiang, Q.-J. Fu, B.-J. Yao, L.-G. Ding, C.-X. Liu, Y.-B. Dong, *ACS Appl. Mater. Interfaces* **2017**, *9*, 36438 – 36446.

[152] Z. Sun, U. Glebe, H. Charan, A. Böker, C. Wu, *Angew. Chem. Int. Ed.* **2018**, *57*, 13810 – 13814; *Angew. Chem.* **2018**, *130*, 14006 – 14010.

[153] B. Yang, L. Leclercq, V. Schmitt, M. Pera-Titus, V. Nardello-Rataj, *Chem. Sci.* **2019**, *10*, 501 – 507.

[154] L. Leclercq, A. Mouret, P. Bauduin, V. Nardello-Rataj, *Langmuir* **2014**, *30*, 5386 – 5393.

[155] B. Yang, G. Douyère, L. Leclercq, V. Nardello-Rataj, M. Pera-Titus, *Catal. Sci. Technol.* **2020**, *10*, 6723 – 6728.

[156] J. Faria, M. P. Ruiz, D. E. Resasco, *ACS Catal.* **2015**, *5*, 4761 – 4771.

[157] N. Xue, G. Zhang, X. Zhang, H. Yang, *Chem. Commun.* **2018**, *54*, 13014 – 13017.

[158] H. Yang, L. Fu, L. Wei, J. Liang, B. P. Binks, *J. Am. Chem. Soc.* **2015**, *137*, 1362 – 1371.

[159] H. Chen, H. Zou, Y. Hao, H. Yang, *ChemSusChem* **2017**, *10*, 1989 – 1995.

[160] M. Zhang, L. Wei, H. Chen, Z. Du, B. P. Binks, H. Yang, *J. Am. Chem. Soc.* **2016**, *138*, 10173 – 10183.

[161] H. Zhao, R. Ran, L. Wang, C. Li, S. Zhang, *AIChE J.* **2020**, *66*, e16239.

[162] F. Peng, J. Xu, X. Zeng, G. Feng, H. Bao, *Part. Part. Syst. Charact.* **2020**, *37*, 1900382.

[163] a) N. Yekeen, M. A. Manan, A. K. Idris, E. Padmanabhan, R. Junin, A. M. Samin, A. O. Gbadamosi, I. Oguamah, *J. Pet. Sci. Eng.* **2018**, *164*, 43 – 74; b) R. Farajzadeh, A. Andrianov, R. Krastev, G. Hirasaki, W. R. Rossen, *Adv. Colloid Interface Sci.* **2012**, *183*, 1 – 13; c) R. Heymans, I. Tavernier, S. Danthine, T. Rimaux, P. Van der Meeren, K. Dewettinck, *Food Funct.* **2018**, *9*, 3143 – 3154.

[164] a) L. K. Shrestha, K. Aramaki, H. Kato, Y. Takase, H. Kunieda, *Langmuir* **2006**, *22*, 8337 – 8345; b) V. Bergeron, J. E. Hanssen, F. Shoghl, *Colloids Surf. A* **1997**, *123*, 609 – 622; c) F. Bauget, D. Langevin, R. Lenormand, *J. Colloid Interface Sci.* **2001**, *239*, 501 – 508; d) C. Blázquez, E. Emond, S. Schneider, C. Dalmazzone, V. Bergeron, *Oil & Gas Sci. Technol.* **2014**, *69*, 467 – 479; Gas Sci. Technol. **2014**, 69, 467 – 479.

[165] G. W. Kauffman, P. C. Jurs, *J. Chem. Inf. Comput. Sci.* **2001**, *41*, 408 – 418.

[166] a) H. Shinto, *Adv. Powder Technol.* **2012**, *23*, 538 – 547; b) J. E. C. Cardona Jaramillo, L. E. K. Achenie, O. A. Alvarez, M. P. C. Bautista, A. F. G. Barrios, *Curr. Opin. Chem. Eng.* **2020**, *27*, 65 – 71.
[167] J. L. Ma, X. Y. Song, B. L. Peng, T. Zhao, J. H. Luo, R. F. Shi, S. L. Zhao, H. L. Liu, *Chem. Eng. Sci.* **2021**, *231*, 116252.
[168] a) T. M. Ruhland, A. H. Gröschel, N. Ballard, T. S. Skelhon, A. Walther, A. H. E. Müller, S. A. F. Bon, *Langmuir* **2013**, *29*, 1388 – 1394; b) S.-L. Zhao, B. C. Zhan, Y.-F. Hu, Z.-Y. Fan, M. Pera-Titus, H. L. Liu, *Langmuir* **2016**, *32*, 12975 – 12985.
[169] a) G. L. Zhao, Y. Li, B. Hong, X. Han, S.-L. Zhao, M. Pera-Titus, H. L. Liu, *Langmuir* **2018**, *34*, 15587 – 15592; b) G. L. Zhao, B. Hong, B. Bao, S.-L. Zhao, M. Pera-Titus, *J. Phys. Chem. C* **2019**, *123*, 12818 – 12826.
[170] H. Fan, A. Striolo, *Soft Matter* **2012**, *8*, 9533 – 9538.
[171] a) H. Fan, D. E. Resasco, A. Striolo, *Langmuir* **2011**, *27*, 5264 – 5274; b) F. Sicard, A. Striolo, *Faraday Discuss.* **2016**, *191*, 287.
[172] a) F. Günther, F. Janoschek, S. Frijters, J. Harting, *Comput. Fluids* **2013**, *80*, 184 – 189; b) F. Günther, S. Frijters, J. Harting, *Soft Matter* **2014**, *10*, 4977 – 4989.
[173] a) S. Razavi, J. Koplik, I. Kretzschmar, *Soft Matter* **2013**, *9*, 4585 – 4589; b) M. Borówko, E. Słyk, S. Sokołowski, T. Staszewski, *J. Phys. Chem. B* **2019**, *123*, 4139 – 4147.
[174] S. Miachon, V. V. Syakaev, A. Rakhmatullin, M. Pera-Titus, S. Caldarelli, J.-A. Dalmon, *ChemPhysChem* **2008**, *9*, 78 – 82.
[175] a) P. Creux, J. Lachaise, A. Graciaa, J. K. Beattie, A. M. Djerdjev, *J. Phys. Chem. B* **2009**, *113*, 14146 – 14150; b) H. Mishra, S. Enami, R. J. Nielsen, L. A. Stewart, M. R. Hoffmann, W. A. Goddard III, A. J. Colussi, *Proc. Natl. Acad. Sci. USA* **2012**, *109*, 18679 – 18683; c) M. Bonn, Y. Nagata, E. H. G. Backus, *Angew. Chem. Int. Ed.* **2015**, *54*, 5560 – 5576; *Angew. Chem.* **2015**, *127*, 5652 – 5669; d) R. R. Feng, Y. Guo, H. F. Wang, *J. Chem. Phys.* **2014**, *141*, 18C507.
[176] a) I. Benjamin, *Annual Rev. Phys. Chem.* **2015**, *66*, 165 – 188; b) K. Piradashvili, E. M. Alexandrino, F. R. Wurm, K. Landfester, *Chem. Rev.* **2016**, *116*, 2141 – 2169.
[177] R. Vácha, S. W. Rick, P. Jungwirth, A. G. F. De Beer, H. B. De Aguiar, J.-S. Samson, S. Roke, *J. Am. Chem. Soc.* **2011**, *133*, 10204 – 10210.
[178] M. Badia, S. El-Moudny, M. Benhamou, M. E. Ossmani, *J. Mol. Liq.* **2017**, *240*, 1 – 13.
[179] a) S. N. Wren, B. P. Gordon, N. A. Valley, L. E. McWilliams, G. L. Richmond, *J. Phys. Chem. A* **2015**, *119*, 6391 – 6403; b) C. Zhu, X. C. Zeng, J. S. Francisco, I. Gladich, *J. Am. Chem. Soc.* **2017**, *139*, 27 – 30; c) C. Zhu, X.-C. Zeng, J.-S. Francisco, I. Gladich, *J. Am. Chem. Soc.* **2020**, *142*, 5574 – 5582.
[180] a) M. Jorge, M. N. D. S. Cordeiro, *J. Phys. Chem. C* **2007**, *111*, 17612 – 17626; b) A. A. Méndez, P. Voyame, H. H. Girault, *Angew. Chem. Int. Ed.* **2011**, *50*, 7391 – 7394; *Angew. Chem.* **2011**, *123*, 7529 – 7532; c) S. Das, S. Behera, S. Balasubramanian, *J. Phys. Chem. Lett.* **2020**, *11*, 2977 – 2982.
[181] Y. Zhang, R. Ettelaie, B. P. Binks, H. Yang, *ACS Catal.* **2021**, *11*, 1485 – 1494.
[182] M. Li, J. Tian, L. Li, A. Liu, W. Shen, *Chem. Eng. Sci.* **2013**, *97*, 337 – 343.

Manuscript received: June 6, 2021
Accepted manuscript online: September 15, 2021
Version of record online: October 1, 2021